A Model to Predict Cell-Mediated Immune Regulatory Mechanisms During Human Infection with *Mycobacterium tuberculosis*[1]

Janis E. Wigginton and Denise Kirschner[2]

A key issue for the study of tuberculosis infection (TB) is to understand why individuals infected with *Mycobacterium tuberculosis* experience different clinical outcomes. Elaborating the immune mechanisms that determine whether an infected individual will suffer active TB or latent infection can aid in developing treatment and prevention strategies. To better understand the dynamics of *M. tuberculosis* infection and immunity, we have developed a virtual human model that qualitatively and quantitatively characterizes the cellular and cytokine control network operational during TB infection. Using this model, we identify key regulatory elements in the host response. In particular, factors affecting cell functions, such as macrophage activation and bactericidal capabilities, and effector T cell functions such as cytotoxicity and cytokine production can each be determinative. The model indicates, however, that even if latency is achieved, it may come at the expense of tissue damage if the response is not properly regulated. A balance in Th1 and Th2 immune responses governed by IFN-γ, IL-10, and IL-4 facilitate this down-regulation. These results are further explored through virtual deletion and depletion experiments. ***The Journal of Immunology*****, 2001, 166: 1951–1967.**

Tuberculosis (TB)[3] has been a leading cause of death in the world for centuries. Today it is the number one cause of death by infectious disease world wide with 3.1 million deaths per year. *Mycobacterium tuberculosis* is not only one of the oldest microbial threats to human health; it is also one of the most formidable, with an estimated one-third of the world population infected.

TB is a unique disease in that 90% of all infections remain latent; however, 5% of infected individuals progress rapidly to primary disease, and 5% of those who initially suppress infection later reactivate developing acute disease sometime during their lifetime (1). An understanding of why some individuals suppress TB infection while others develop active disease is still forthcoming. It is believed that host immune mechanisms are crucial in determining these alternative disease trajectories.

An enormous body of literature exists regarding individual elements of both bacterial mechanisms and the immune response to TB; however, little is known about combined interactions or the balance between these processes. Additionally, data derived from murine models may not always accurately represent or predict the human response, given that latent tuberculosis is common in humans but seldom seen in mice. To this end, we have developed a virtual model of the human cell-mediated immune response to infection with *M. tuberculosis* that incorporates major elements of the host immune response critical to the course of TB infection, namely, macrophages, T cell populations, and cytokine mediators together with the pathogen *M. tuberculosis*. We estimate parameters from current literature and explore others that are not presently known. We then use the model to perform a number of virtual experiments predicting elements of the system that contribute to the different disease outcomes. This model makes specific predictions concerning the roles of IL-10, IL-12, IFN-γ, and IL-4 and describes key elements of cell-mediated immunity that lead to latency or active disease.

Primary TB, the response following the first exposure to *M. tuberculosis*, usually develops in the alveoli of the lung. When droplets containing *M. tuberculosis* are inhaled, the bacteria are ingested by resident alveolar macrophages and begin to multiply (2). Alveolar macrophages are an ideal target for *M. tuberculosis*. In their resting state, not only are alveolar macrophages poor at destroying mycobacteria but *M. tuberculosis* can also inhibit their ability to kill phagocytized bacteria, most likely by preventing phagosome-lysosome fusion (3–5). Clearance of resident bacteria by alveolar macrophages is dependent on the presence of lymphocytes as well as activation by IFN-γ, released by Th1 cells and other cells of the immune response (such as NK cells and $CD8^+$ T cells) that migrate to the site of infection in response to chemotactic signals generated by infected macrophages (6). If the macrophage does not receive sufficient stimulation for activation, it is unable to clear its resident bacteria. These chronically infected macrophages eventually either die due to a large number of resident bacteria or are destroyed by a CTL response.

Naive $CD4^+$ T cells are most probably activated at the site of infection and in the neighboring lymph nodes. On the basis of available data, we assume that naive $CD4^+$ T cells are first activated into a Th0 state. These Th0 cells differentiate into either Th1 or Th2 cells depending on signals received. A large amount of data support the role played by cytokines in this process (7–11), and thus our model focuses on the role of cytokine signals in differentiation; however, present studies by our group are exploring other differentiation theories.

Department of Microbiology and Immunology, University of Michigan Medical School, Ann Arbor, MI 48109

Received for publication August 17, 2000. Accepted for publication November 13, 2000.

The costs of publication of this article were defrayed in part by the payment of page charges. This article must therefore be hereby marked *advertisement* in accordance with 18 U.S.C. Section 1734 solely to indicate this fact.

[1] This work was supported by National Institutes of Health Grant #HL62119-01 and The Whitaker Foundation.

[2] Address correspondence and requests for reprints to Dr. Denise Kirschner, Department of Microbiology and Immunology, University of Michigan Medical School, Ann Arbor, MI 48109-0620. E-mail address: kirschne@umich.edu

[3] Abbreviations used in this paper: TB, tuberculosis; BAL, bronchoalveolar lavage; MOI, multiplicity of infection; BCG, bacillus Calmette-Guérin; PPD, purified protein derivative.

0022-1767/01/$02.00

T cells are responsible for killing infected macrophages that are unable to destroy their resident bacteria. This is accomplished via a Fas-Fas ligand apoptotic pathway (by $CD4^+$ T cells (12–14)) and via other cytotoxic mechanisms such as granules and perforins (by $CD8^+$ and possibly $CD4^+$ T cells (14–18)). Bacteria are either killed when their host cell is destroyed or released, becoming, at least temporarily, extracellular. These bacteria may either infect resting macrophages or be ingested (and killed) by activated macrophages. Conversely, intracellular mycobacteria appear to have the ability to down-regulate apoptosis of their host macrophages which may prolong their survival within the protective intracellular environment (19–21).

During the course of TB, severe tissue damage may occur as a consequence of the immune response. This response may be mediated primarily by T cells and activated macrophages. Thus, although it is clear that the Th1-type response plays an important role in immunity to *M. tuberculosis*, it must also be carefully regulated to ensure that severe tissue damage does not occur. Down-regulation of an ongoing Th1-type response is achieved via the production of IL-10 and other cytokines that deactivate macrophages. If down-regulation is improperly achieved, then either the disease may not be arrested or extensive tissue damage can accompany latent infection.

The Host-Pathogen Interaction with *M. tuberculosis*

Within the TB literature, alternate theories as to why individuals have different disease outcomes after exposure to *M. tuberculosis* have been proposed. Given the abundance of data pointing to the role of various host susceptibility and resistance genes, it seems clear that a genetic component exists (22, 23). Nonetheless, a number of theories assert that specific components of the host immune response play the primary role in determining resistance to TB. There may exist a link between the genetic and immune components; however, this study explores the immune response at the cellular level. Several of the immune theories focus on the central role of Th1/Th2 cross-regulation. In particular, it has been hypothesized that there is a switch from a Th1- to a Th2-dominant cell-mediated immune response leading to active disease as is seen in other infections such as *Leishmania*, schistosomiasis, and HIV. However, attempts at isolating Th2 cells and Th2-type cytokines from the site of infection have not always been successful (24–26). In fact, in several studies IL-4 expression in samples from infected individuals was shown to be lower than in those from uninfected controls (27–29). This would seem to indicate that the role played by Th1/Th2 immunity may not be a simple one. A second hypothesis is that a true switch from a Th1 to a Th2 response does not necessarily occur but, instead, that the relative strength of the Th1 response determines latency or active disease in TB (*cf.* Refs. 30–32). We explore each of these hypotheses with the model.

Although many aspects of the host-pathogen interaction with *M. tuberculosis* have been studied individually, there are no studies that examine the combined interactions of known elements of the immune response and therefore no effective methods for assessing the role that system-wide dynamics (such as Th1/Th2 cross-regulation) may play in determining the course of TB infection. If we are to understand the events that occur in the development and evolution of the immune response to TB, it is necessary to understand what elements contribute to the interactions in this dynamic system. Thus, our goal is to develop a model that integrates known features of the host-pathogen interaction and then use it to test theories regarding the role of specific cytokines in infection outcome, a switch from Th1 to a Th2 response, and elements of the system that lead infection to disease or latency. We can also assess how extensive tissue damage may occur even if latency is achieved.

Virtual Model of the Immune Response to *M. tuberculosis*

Our system is developed to model human TB at the site of infection in lung tissue. Our "reference space" for the model is bronchoalveolar lavage (BAL) fluid, and we measure all cells and cytokines in units per milliliter of BAL. Although the possibility exists that the quantitative response differs between the airspace and the interstitium, we rely on the acceptance of BAL as a qualitative predictor of lung environment (33, 34). We also note that in at least one study, BAL has been shown experimentally to reflect cell populations in tissue granulomas, as well as local cytokine quantities (35). We outline the major interactions among two bacterial populations, six cell populations, and four cytokines. For this first modeling attempt, we do not include every cell potentially involved (i.e., NK cells, eosinophils, . . .) or every relevant cytokine (i.e., IL-2, TGF-β, TNF-α, . . .). Our first goal is to develop a model that represents the basic processes of the immune response to TB. This model can then serve as a template on which to add other cells, cytokines, and interactions, as new data warrant, to determine how their presence augments the system dynamics. A complete mathematical description of the model is presented in *Appendix*; however, a conceptual description is given below. Accompanying each description is a diagram summarizing model features.

Macrophages

Three populations of macrophages are included in the model: resting, activated, and chronically infected macrophages, denoted respectively by $M_R(t)$, $M_A(t)$, and $M_I(t)$.

Resting macrophages. Resting macrophages ($M_R(t)$) are the class of macrophages that may present Ag, phagocytize and kill bacteria, and secrete cytokines; however, they are less efficient at each of these processes than activated macrophages and therefore play a different role in the course of TB infection. Resting macrophages can become activated in response to IFN-γ together with exposure to bacterial Ag (36–38). Resting macrophages can also become chronically infected.

Activated macrophages. We consider a macrophage activated if it is in a state in which it can efficiently phagocytize and kill mycobacteria. Activated macrophages ($M_A(t)$) are effective at killing *M. tuberculosis* because they are more efficient at phagosome-lysosome fusion than resting macrophages and also produce oxygen radicals, NO, and other antimicrobial molecules. Although activated macrophages play a crucial role in suppression of *M. tuberculosis* infection, one consequence of their killing activity is some degree of tissue damage. Therefore, macrophage activation must be tightly controlled. The main cytokine that down-regulates activated macrophages is IL-10. It down-regulates MHC II expression and NO production and overrides the antimycobacterial effects of IFN-γ on macrophages (39–41). Activated macrophages deactivate over time when they are not given sufficient stimuli (42).

Chronically infected macrophages. The chronically infected macrophage population ($M_I(t)$) represents an important class of macrophages. In this model, they contain a large a number of bacteria but have not received adequate stimuli for activation (facilitated by bacterial factors). Such macrophages eventually lose the capacity to become activated and thus are unable to clear their bacterial load (4, 5, 42, 43).

Thus, chronically infected macrophages are the key reservoir

for *M. tuberculosis*. Bacteria within chronically infected macrophages continue to multiply; if this proliferation is unchecked by a cytotoxic T cell response, the number of *M. tuberculosis* within a chronically infected macrophage may approach the limit of the capacity of the macrophage to sustain bacteria (i.e., the maximal multiplicity of infection (MOI)). If the number of bacteria within a macrophage reaches this capacity (denoted by N), the macrophage may be killed and the bacteria released into the extracellular environment. Alternatively, the bacteria may respond by slowing their growth and maintaining the viability of their host cell (44). A chronically infected macrophage may also be lysed by $CD4^+$ or $CD8^+$ T cells via apoptotic or cytotoxic mechanisms (13–17). Finally, we note that *M. tuberculosis* appears to have the capacity to down-regulate T cell-mediated lysis of its host macrophage, either by down-regulating receptor expression on the macrophage or by other unknown mechanisms (19–21).

Cytokines

We model four key cytokines known to play a key role in the course of human TB. Their principal effects included in the model result in cellular activation, deactivation, and differentiation.

IL-10. IL-10 plays a number of important roles in down-regulating an active immune response in TB, including deactivation of macrophages (39, 40, 45), inhibition of T cell proliferation (45, 46), and suppression of cytokine production by T lymphocytes (46–49). IL-10 is produced primarily by macrophages in response to infection with *M. tuberculosis* (50–52) and is also produced in smaller quantities by Th2 lymphocytes. Additionally, in humans, who differ from mice, Th0 and Th1 lymphocytes also produce IL-10, in response to IL-12 (53–55). This difference in IL-10 production may be an important place where murine models cannot accurately predict the disease outcome in humans; however, we are able to include this feature in our virtual model.

IL-12. IL-12 is a key Th1-type cytokine. Produced by activated and infected macrophages in response to Ag stimulation (56–60), IL-12 regulates the ongoing immune response, primarily by inducing differentiation of Th0 lymphocytes to Th1 lymphocytes (61–63), but also by enhancing the production of IFN-γ (64). Macrophage production of IL-12 is considerably enhanced when the macrophage is primed with IFN-γ (56, 60); however, production is simultaneously inhibited by IL-10 (56, 59, 60).

IL-4. IL-4 is considered to be the prototypical Th2 cell cytokine. It is the cytokine that governs differentiation of Th0 cells to Th2 cells. As discussed above, the role of IL-4 in the immune response to TB is controversial. It is involved in down-regulating and opposing the development of a Th1-type cell response by inhibiting Th0 to Th1 differentiation (11, 65).

IFN-γ. IFN-γ, a Th1-type cytokine, is key to the development of an effective cell-mediated response to *M. tuberculosis*. IFN-γ activates resting macrophages, enhancing their ability to effectively clear pathogens and also to release cytokines (36, 38, 66). IFN-γ is also involved in the process of T cell differentiation by enhancing the rate of Th0 to Th1 differentiation and by overriding opposition by IL-4 to this process (11, 65).

$CD4^+$ T lymphocytes

We include in the model known interactions for $CD4^+$ T cells. *CD4*$^+$ T lymphocytes play two main roles in TB infection: the first is in the production of cytokines that govern the cell-mediated immune response; the second is elimination of infected macrophages via apoptosis.

Bacterial subpopulations

We model two distinct bacterial subpopulations according to their extracellular or intracellular status. Differences in bacterial location (intracellular or extracellular) dictate growth rates and their role in soliciting the immune response and thus may be important in infection dynamics. To account for these differences, we represent the population of bacteria that resides within the protected environment of the chronically infected macrophage as intracellular TB, denoted by $B_I(t)$. Bacteria found anywhere except within chronically infected macrophages are considered to be extracellular TB, denoted by $B_E(t)$. Bacteria that are found within activated macrophages would be considered extracellular bacteria ($B_E(t)$). This distinction allows extracellular bacteria to be vulnerable to direct killing via activated macrophages, whereas intracellular bacteria may be killed only if the infected macrophage in which they reside is lysed.

Results

To explore the model, we develop a mathematical system representing the terms in Figs. 1–4 and then estimate the associated parameters from literature (summarized in *Appendix*). We then simulate the model by solving the differential equations using an appropriate numerical method. We discuss below the results of the computational experiments in three general areas: disease outcome experiments; damage parameter experiments; and virtual deletion and depletion experiments.

The negative control, if there is no *M. tuberculosis* present in the system, should yield a result with resting macrophages at equilibrium (3×10^5/ml) and all other populations and cytokines at zero. The model easily satisfies the negative control experiment (data not shown). The model also indicates that it is possible to be exposed to an initial bacterial inoculum and then clear infection with no memory of that response (i.e., purified protein derivative (PPD) negative) (data not shown). This outcome may indeed be plausible, given that it is thought that only 30% of individuals exposed to TB become infected (i.e., PPD positive) (1).

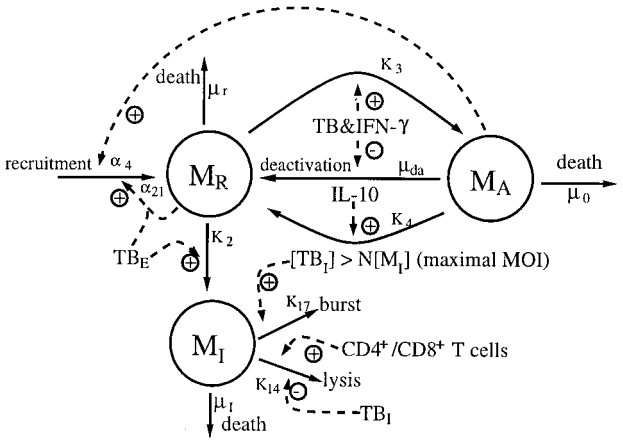

FIGURE 1. Model diagram of macrophage interactions (see Equations 1–3 in *Appendix*). Three populations of macrophages are included in the model: resting, activated and chronically infected macrophages, denoted, respectively, by $M_R(t)$, $M_A(t)$, and $M_I(t)$. The alphanumeric and Greek symbols indicate the rates at which these processes occur. Solid arrows indicate alterations of cell state; dashed arrows indicate rate modifiers. Plus sign indicates up-regulation; minus sign indicates down-regulation. This figure is coupled to Figures 2, 3, and 4 via T cell, cytokine, and bacterial interaction terms.

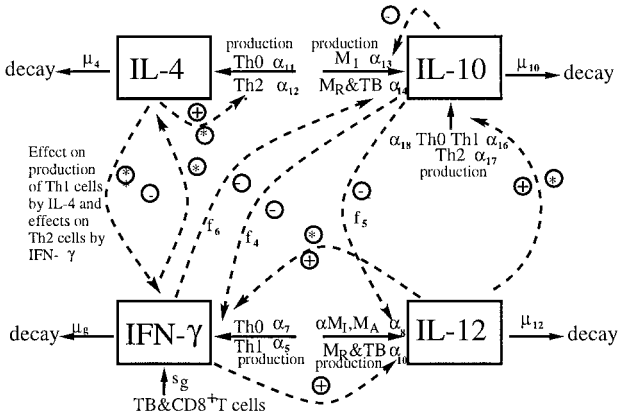

FIGURE 2. Model diagram of cytokine interactions (see Equations 7–10 in *Appendix*). Four cytokines are tracked in the model: IL-12, IL-10, IL-4, and IFN-γ. The alphanumeric and Greek symbols indicate the rates at which these processes occur. The ∗ indicates that multiple parameters control the process. Long dashed arrows indicate regulation of other cytokines; short arrows indicate production by cell type listed. Plus sign indicates up-regulation; minus sign indicates down-regulation. This figure is coupled to Figures 1, 3, and 4 via T cell, macrophage, and bacterial interaction terms.

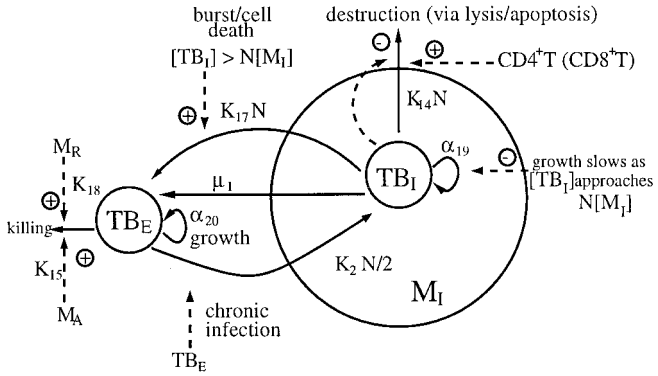

FIGURE 4. Model diagram of bacterial interactions (see Equations 11 and 12 in *Appendix*). Two bacterial populations are tracked: intracellular bacteria (B_I) and extracellular bacteria (B_E). The alphanumeric and Greek symbols indicate the rates that these processes occur. Solid arrows indicate alterations of cell state; dashed arrows indicate rate modifiers. Plus sign indicates up-regulation; minus sign indicates down-regulation. This figure is coupled to Figures 1, 2, and 3 via T cell, macrophage, and cytokine interaction terms.

Obtaining different disease trajectories

The main goal of this theoretical study is to explore what elements of the host-pathogen interaction in infection with *M. tuberculosis* lead the system to suppression or active disease. Thus, the system should exhibit both a suppression response leading to latency and a response that fails to suppress infection leading to acute, primary disease. Figs. 5–8 present representative simulations of the virtual infection model for two given sets of parameter values, one leading to latency and the other leading to active disease. We show the latent and disease outcomes together for comparison.

Latency. Figs. 5*A*–8*A* present the latency results of a virtual human infection. During latency, the extracellular bacteria load is almost zero (Fig. 5*A*). Both intracellular and extracellular bacteria undergo minor oscillations over time, which indicates that rounds of bacterial growth may occur during the lifetime of latency. Also, minor oscillations of the immune response occur in response to oscillations in bacterial load. A key point is that whereas extracellular bacterial load is almost zero, the intracellular bacterial load is higher. These intracellular bacteria reside within a small number of chronically infected macrophages, $<3 \times 10^3$/ml (Fig. 6*A*). This may explain why it is difficult to detect bacteria in latent infection if tissue samples miss the small number of chronically infected macrophages. The model predicts that it takes on average 1 year to achieve latent equilibrium, although by 100 days infection is controlled.

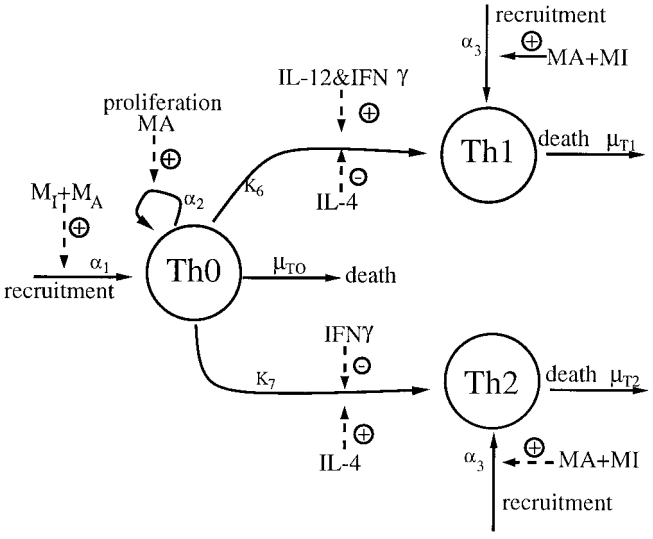

FIGURE 3. Model diagram of T cell interactions (see Equations 4–6 in *Appendix*). Three T cell populations are followed: T_0, T_1, and T_2 cells. The alphanumeric and Greek symbols indicate the rates that these processes occur. Solid arrows indicate alterations of cell state; dashed arrows indicate rate modifiers. Plus sign indicates up-regulation; minus sign indicates down-regulation. This figure is coupled to Figures 1, 2, and 4 via macrophage, cytokine, and bacterial interaction terms.

Fig. 6*A* presents the corresponding macrophage results for latency. Resting macrophages in the absence of infection maintain an equilibrium near 3×10^5 cells/ml (67–70). Despite their continual recruitment, the drop in resting macrophages during infection indicates a gain (transfer) to either the activated or infected cell classes. Activated macrophages parallel that of the *M. tuberculosis* populations, and oscillate in response to replication. During latency, the final activation level is low, indicating that there may be low level background immunity present to respond to persister bacteria.

The cytokine IL-4 is extremely low during latency, and IFN-γ is present but controlled by IL-10 which is present in slightly a higher concentration than is found in active disease (Fig. 7*A*). Predictions from the model for levels of IFN-γ and IL-10 in active vs latent disease correlate well with results obtained from a recent study measuring in vitro cytokine production by $CD4^+$ T cell clones obtained from BAL of human subjects with active and latent TB (71). Additionally, predicted ranges from our model for levels of IL-10, IL-12, and IFN-γ all correspond to a number of studies quantifying cytokine levels at the site of disease in TB (50, 72, 73). Levels predicted for IL-4 are lower than those reported by some studies from active TB patients (e.g., 12–1032 pg/ml in Ref. 72) but higher than in other studies that report undetectable levels of IL-4 at the site of infection (50). Thus, our model predictions are within experimentally obtained ranges, which exhibit wide variability. We discuss in subsequent sections how an intrinsic variability in IL-4 production may be important in the course of TB. Finally, Fig. 8*A* shows that during latency, Th1 and Th2 cells are

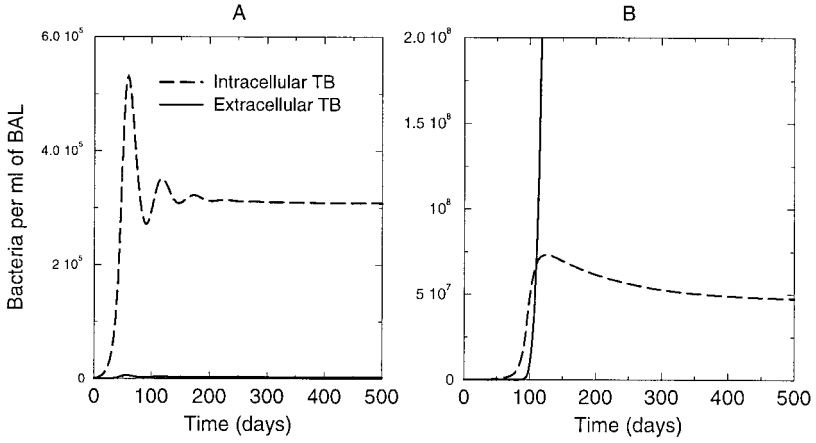

FIGURE 5. Model simulation results for *M. tuberculosis*. *A*, Results when latency is achieved; *B*, results of acute infection. Units are bacteria per milliliter of BAL. The *y*-axis scales are different in *A* and *B*, because there are order of magnitude differences in bacterial amounts.

present in similar numbers, whereas Th0 cells are present in higher numbers as an available source.

Primary disease. Figs. 5*B*–8*B* present active disease results of a virtual human infection. The extracellular bacterial load grows exponentially during primary acute infection once the intracellular bacterial load reaches the maximal capacity of chronically infected macrophages (Fig. 5*B*). This reflects results from mouse models with large bacterial loads at end-stage disease (25, 26, 74, 75). The level of infected macrophages is 600 times that which occurs during latency, and the level of activated macrophages is 20 times that during latency. This large activated macrophage response implies that tissue damage will likely be severe. We also note that Th2 cells correspondingly are present at levels 3 times greater than that of Th1 cells and 60 times greater than during latency (in Fig. 7, compare *A* with *B*). T lymphocyte-macrophage ratios and absolute cell counts for this and other activation scenarios generated by our model also correspond well with human clinical observations (67, 68, 70).

In the model, IL-4 is present during active infection, although its concentration is low enough that it may be undetectable (Fig. 7*B*). In one clinical study examining granulomas from patients with acute TB, IL-4 mRNA and Th2 cells were present, but their presence or absence did not correlate with clinical outcome (29). However, several other studies have reported marked correlations between IL-4 expression and clinical outcome (76, 77). Our results provide a possible explanation for these contradictory findings, namely, that active disease can occur even when IL-4 levels are low if other cell-mediated immune mechanisms are compromised (We discuss further this variability in IL-4 in the next section.). Levels of IL-10 are approximately the same, but slightly lower than seen during latency, as has also been seen in recent experimental results (71). This follows because arresting the immune response during active disease could be detrimental. Also, IFN-γ and IL-12 production are both considerably enhanced in active vs inactive disease. These predictions also correlate well with observed results in human subjects (68, 78).

Differences in disease outcomes

Parameters that govern the rates and behavior of interactions in the model may change from individual to individual and over time within an individual. The model reveals that changes in only certain parameters lead to the different disease outcomes in our virtual experiment, either latency or active disease (see Figs. 5–8). Table I summarizes the parameters in the model that affect such changes.

Our primary finding is that the rate of T cell killing (via cytotoxic or apoptotic mechanisms) of chronically infected macrophages (k_{14}) governs infection outcome. High efficiency of T cell killing of infected cells, and consequently bacteria, maintains latency, whereas lower efficiencies lead to active disease. An important aspect of this result is the tradeoff between this rate (k_{14}) and two others: the rate at which activated macrophages kill bacteria (k_{15}); and sources of IFN-γ from NK or $CD8^+$ T cells (s_g). This follows given that it is IFN-γ that activates macrophages and would thus indirectly effect bactericidal activity.

When the value for the extra source of IFN-γ (s_g) is decreased, greater efficiency in T cell killing of bacteria is required to maintain the latent state (i.e., k_{14} must increase). Conversely, if IFN-γ levels are sufficient, the efficiency of T cell cytotoxicity required to

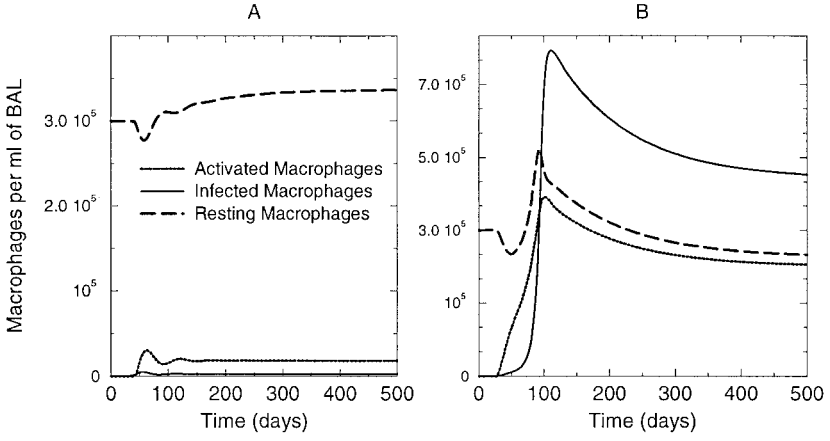

FIGURE 6. Model simulation results for macrophages. *A*, Results when latency is achieved; *B*, results of acute infection. Units are macrophages per milliliter of BAL.

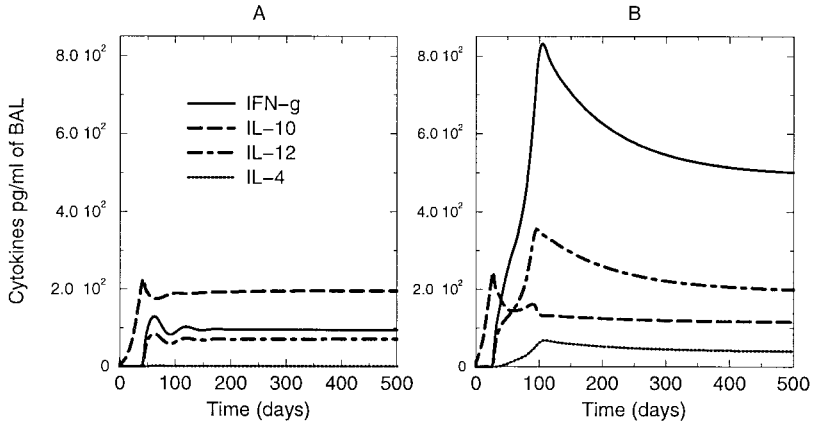

FIGURE 7. Model simulation results for the cytokines. *A*, Results when latency is achieved; *B*, results of acute infection. Units are cytokine (picograms) per milliliter of BAL.

maintain the latent state lowers (i.e., decrease in k_{14}). Fig. 9 presents different disease trajectories as k_{14} is varied over a biologically reasonable range.

A similar tradeoff exists between the rate of activated macrophage killing of bacteria and T cell cytotoxicity; if macrophage function is compromised, the T cell response must be more potent to control infection. However, when the rate of activated macrophage killing of bacteria is considerably increased (beyond values estimated from experimental data), latency is consistently achieved, even for severely compromised T cell function. Each of these results indicate that levels of IFN-γ from sources other than $CD4^+$ T cells, as well as adequate macrophage function, can determine infection outcome. These results also imply that $CD8^+$ T cells are likely key factors in the immune response to TB.

Table I summarizes several other factors that contribute significantly to the outcome of *M. tuberculosis* infection. First, even in the presence of adequate T cell and macrophage killing, high production of IL-4 by Th0 cells (α_{11}) may be associated with a shift from latency to active disease. Although IL-4 is frequently not detected in pleural fluid or BAL samples either from mice or from humans (27, 50, 68, 79), several recent human studies have found evidence that enhanced IL-4 expression may be correlated with active TB. In particular, markedly elevated concentrations of IL-4 in BAL fluid taken from patients with active TB have been reported (72, 73). Another study found IL-4 mRNA expression from PBMCs to be significantly greater in subjects with active tuberculosis relative to matched tuberculin-positive control subjects (76). Yet another recent report indicates that increased production of IL-4 is particularly elevated in patients with cavitary TB (77). Our results suggest that this natural variability in IL-4 expression within human subjects may indeed be significant in determining clinical outcome in TB.

Second, our results confirm that macrophages are key to determining disease trajectories. Parameters that govern macrophage activation (k_3), macrophage death rates (μ_r), and macrophage infection rates (k_2) all drive the system to either latency or active disease depending on their values (see Table I).

Damage parameters

Tissue damage incurred by the immune response as a consequence of immune protection can be a significant factor in the suppression or progression of tuberculosis. Thus, it is desirable not only to suppress bacterial infection but also to do so in the most efficient manner with respect to the magnitude of effector cell responses. A number of parameters in our model are intimately related to tissue damage as defined by the effector cell activity to TB killing ratios present during the response. In particular, variations in some parameters produce very little difference in bacterial load but can significantly increase tissue damage. These damage parameters are listed in Table II. Specifically, our model predicts that either an increased production of IFN-γ (by Th0 (α_7) or Th1 (α_5) cells) beyond a lower limit that would already control infection or a slower decay rate (μ_{ig}) exacerbate damage. Also, if the rate of IL-4 decay increases or IL-10 production by resting macrophages (α_{13}) decreases, greater damage will occur. These results illustrate the intricate balance that exists between down-regulatory and up-regulatory immune components; immune activation is clearly required for suppression of infection; however, when bacterial loads are adequately reduced, down-regulatory signals (such as IL-4 and IL-10) act to minimize tissue damage.

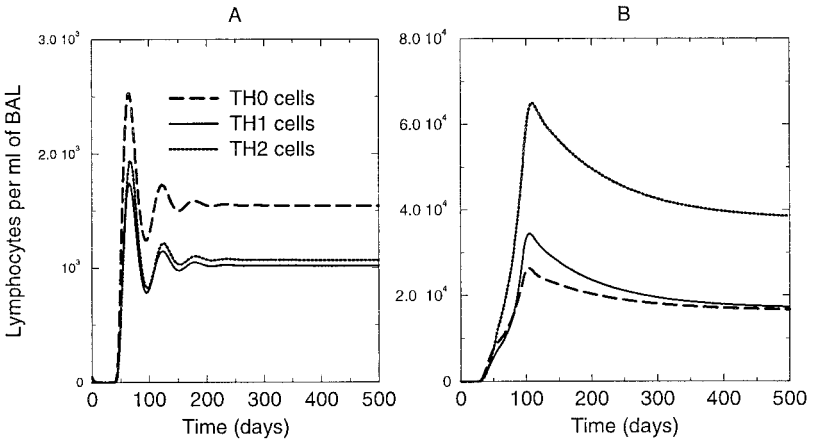

FIGURE 8. Model simulation results for the $CD4^+$ T cells. *A*, Results when latency is achieved; *B*, results of acute infection. Units are T cells per milliliter of BAL. The *y*-axis scales are different in *A* and *B*, because there are order of magnitude differences in lymphocyte counts.

Table I. *Parameters that lead to disease from latent state*[a]

Symbol	Latency	Disease Occurs	Explanation of Parameter	Units
α_{11}	0.03	Increase	IL-4 produced by T_0 cell	pg/T_0 day
μ_r	0.138	Increase	Rate of M_R death	1/day
k_3	0.04	Decrease	Maximal M_R activation	1/day
k_2	0.9	Increase	Maximal M_R chronic infection	1/day
k_{14}			Maximal T cell killing of M_I	1/day
if $k_{15} \leq 4.5 \times 10^{-7}$	1.3	Decrease	(k_{15}) is rate B_E killed by M_A	ml/M_A day
if $k_{15} > 4.5 \times 10^{-7}$	Any value	Never		
k_{14}			Maximal T cell killing of M_I	1/day
if $s_g = 0.7$	1.3	Decrease	(s_g) is rate IFN-γ by NK and $CD8^+$	pg/ml day
if $s_g = 0.6$	1.4	Decrease		
if $s_g = 0.5$	1.5	Decrease		
if $s_g = 0.4$	1.65	Decrease		
if $s_g = 0.3$	1.94	Decrease		
if $s_g = 0.2$	2.35	Decrease		
if $s_g = 0.1$	3.35	Decrease		

[a] Latency threshold values are the values at which changes (increase or decrease) lead to active disease.

For long term reactivation in TB to occur in the virtual human infection model, one or more of the parameters listed in Table I must change from their latent value to a disease value over time. This could happen over a short time period if some exogenous factors are imposed, such as immunosuppressive therapy. Alternatively, the changes could happen over a long time frame representing aging or the development of a disease that has a long incubation or infection period (such as AIDS), both of which predispose a latently infected person towards reactivation. The model can capture each of these features based on changes in parameters (or in combinations of them) that govern the immune response. However, the model indicates that unless some element(s) of the system changes over time, long term reactivation cannot be achieved. Fig. 10 shows the results of altering immune response parameters (α_1, α_3, α_2, s_g) that govern T cell recruitment and growth, and production of IFN-γ from sources other than Th1 cells. The data are presented as effects on the bacterial populations showing how both short and long term loss of latency occurs when these parameters are altered. This example would mimic HIV infection and progression with the loss of T cell immunity over time (Fig. 10*B*).

Virtual deletion and depletion experiments

The power of the model we have developed is that it now can be manipulated in a variety of ways to ask questions about interactions and rates within the system. By doing so, we can explore experimental outcomes on a scale that would be difficult, if not

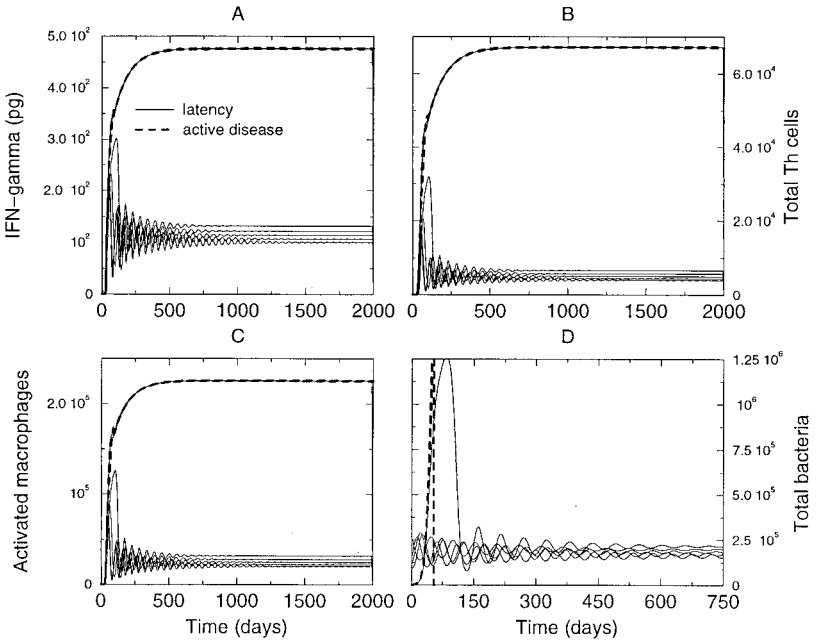

FIGURE 9. Parameter values dictate latency or active disease. We vary the parameter that governs T cell-mediated apoptosis (k_{14}). We perform 10 experiments choosing 10 different values for k_{14} over an estimated range of values, from 0.1 to 2.0. *D* shows the total bacterial population with the trajectories leading to latency (the solid bottom curves in the panel) and trajectories growing exponentially leading to active disease (dashed lines). Corresponding values are shown for other populations in the other three panels. Higher values for k_{14} lead to latency; lower values lead to active disease. *A*, Representative cytokine, IFN-γ; *B*, total $CD4^+$ T cell population; *C*, activated macrophages. All units are per milliliter of BAL.

Table II. *Damage parameters are those parameters that lead to exacerbated effector cell functions beyond what is needed to suppress infection*[a]

Symbol	Range Explored	Maximal Damage Occurs in	Explanation	Units
α_1	(0.0, 0.5)	Low range	T_0 recruitment by M_A and M_I	T_0 /MΦ day
α_5	(0.0, 0.2)	High range	IFN-γ production by T_1	pg/T_1 day
α_7	(0.0, 0.2)	High range	IFN-γ production by T_0	pg/T_0 day
α_{13}	(0.0, 0.1)	Low range	IL-10 production by M_R	pg/M_R day
μ_{ig}	(0.0, 10.0)	Low range	Decay rate, IFN-γ	1/day
μ_{i4}	(0.0, 10.0)	High range	Decay rate, IL-4	1/day

[a] Each parameter was explored over a broad range, and indicated is the portion of the range where damage can occur.

presently impossible, to analyze with other approaches. For example, we can perform both virtual deletion and depletion experiments in this human model for comparison with known experimental results in mice as well as perform new experiments. Deletion experiments mimic knockout (disruption) experiments whereby we remove an element from the system at day 0, before any infection is imposed into the system. This type of analysis allows us to elaborate which system elements control the establishment latency. Second, we can simulate depletion experiments by setting the relevant parameters to zero after the system has already achieved latency. These depletion experiments mimic, e.g., the addition of Ab that can neutralize all available cytokine of one type. This analysis allows us to determine what elements control maintenance of latency.

Virtual deletion experiments. We use our model to make predictions on cytokine deletion experiments; three cytokines, IFN-γ, IL-12, and IL-10, are explored. When the model is initiated with all IFN-γ parameters and rates set to zero, we simulate a IFN-γ deletion model. The results indicate that the system goes to active disease within 100 days (data not shown). This parallels results in both IFN-γ knockout murine experiments where the mice die of active TB within a short time (25, 74) and results in studies of BCG immunization of two children with a rare genetic mutation for the IFN-γ receptor gene who suffered disseminated disease (80, 81). Similar results are obtained with the model for IL-12 deletion (data not shown). Experimental data on IL-12 indicate that murine IL-12-knockouts exhibit a lack of both *Th*1 and *Th*2 cytokines in response to infection with BCG, with an absence of IL-12 and IFN-γ, and no increases in IL-4 relative to control C57BL/6 mice. Additionally, knockout mice exhibit severely impaired tissue-inflammatory responses, with strikingly lower numbers of lymphocytes throughout the course of infection and impaired recruitment of alveolar macrophages (26, 75). Our model anticipates each of these results and, additionally, predicts that at least in humans, IL-10 levels would not be significantly different, even in the absence of IL-12.

Lastly, we explore IL-10 deletion. In this scenario, our results indicate that although the bacterial levels are lower than in the positive control (Fig. 5*A*), suppression of infection occurs in an oscillatory manner. Cells and cytokines cycle about the average value of 2×10^5/ml of BAL (see Figs. 5–8) with a variance of 10^5 (data not shown). Thus, IL-10 is a necessary regulatory cytokine for achieving steady state. Furthermore, although bacterial levels are lower, IFN-γ production has not increased. This finding is consistent with observations in murine IL-10 knockouts that noted this same phenomenon (82). We explore this further using virtual depletion experiments.

Virtual depletion experiments. We next use our model to make predictions on cytokine depletion experiments; we again explore the three cytokines, IFN-γ, IL-12, and IL-10. To perform these experiments, model simulations are done with parameters that lead the system into latency. Then, we deplete all cytokine from the system. First, IFN-γ depletion reveals that although the system eventually progresses to active disease, it happens over a long time frame (~500 days; data not shown). This indicates that once the system has achieved latency, a small but insufficient number of activated macrophages present at the time of IFN-γ-depletion lead to a slow but eventual progression to active disease. For the IL-12 depletion experiments, the results are quite different. Here, the system is still able to maintain latency, although the bacterial load is much higher and the level of cellular activation is lower (data not shown). This implies that the system can more easily lose latency with minor changes to other parameters in the system.

Finally, we explore IL-10 depletion (Fig. 11). When IL-10 is depleted from the system after latency is achieved, there is an abrupt increase in macrophage activation and IFN-γ production that leads to a cascade of events suppressing bacterial numbers to

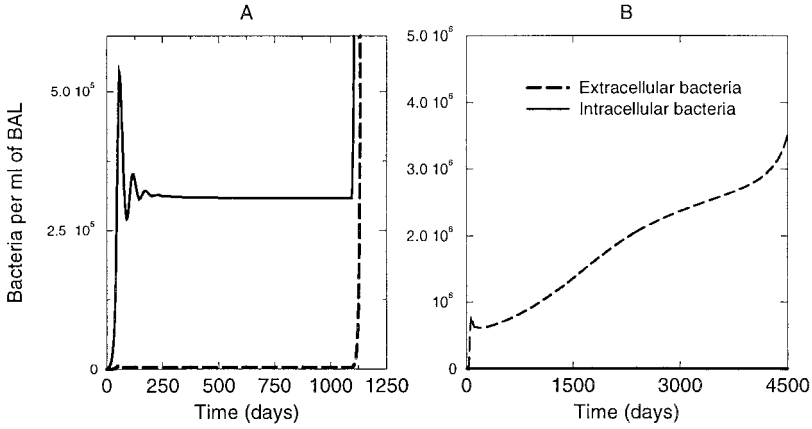

FIGURE 10. Reactivation. Intracellular and extracellular *M. tuberculosis* populations are shown per milliliter of BAL. *A*, Short term reactivation that occurs when the immune system is altered abruptly on changing the parameters that govern T cell recruitment (α_1, α_3), growth (α_2), and other sources of IFN-γ (s_g); *B*, long term reactivation if the same parameters decrease in efficiency over time, indicating a slow loss of immune function.

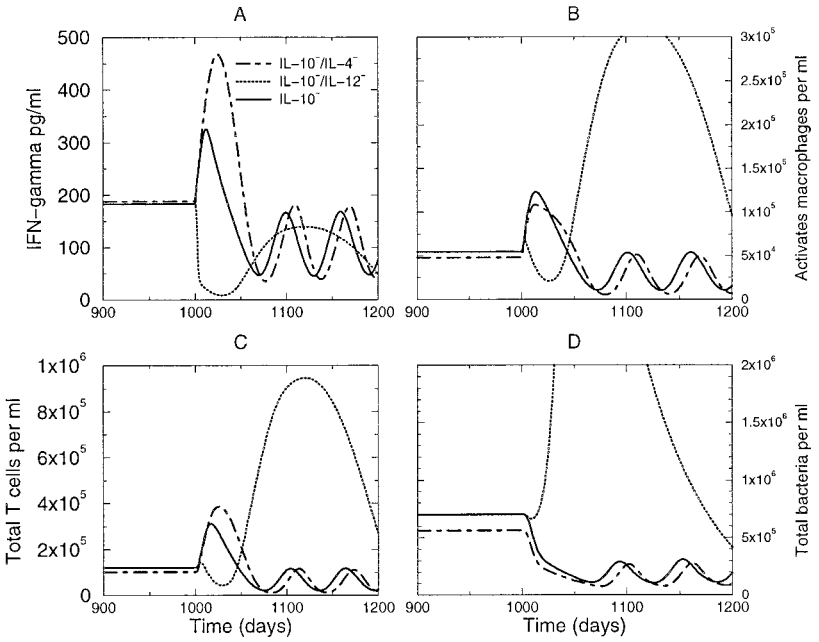

FIGURE 11. IL-10 depletion experiments. Three depletion experiments are performed and shown for four representative populations over time. *A*, Effects on IFN-γ when IL-10 only (solid line), IL-10 and IL-4 (dashed line), and IL-10 and IL-12 (dotted line) are each depleted; *B*, effects on the activated macrophage population; *C*, effects on the total T lymphocytes; *D*, total bacterial population. In each case, the system was in latency before the depletion was performed. Units are per milliliter of BAL.

one-third of what is observed during latency (compare Fig. 5*A* with Fig. 11*D*). Once the bacterial load drops, the immune response returns to equilibrium by 100 days at levels one-half to one-third of previous latency values (Fig. 11). This appears to be driven by a large increase in IL-4 (3 times its level), presumably compensating for the lack of IL-10. A second virtual experiment whereby we deplete both IL-10 and IL-4 confirms this, because the bacterial load is still suppressed after 100 days; however, the amount of immune activation and thus tissue damage is twice as high. In this case, it is the lack of Ag stimulation that accounts for the eventual down-regulation of the system.

Our results from IL-10 deletion experiments did not indicate an increased production of IFN-γ; thus, the increase in IFN-γ when IL-10 is depleted was somewhat unexpected. Exploring further, we simultaneously depleted IL-10 and IL-12, and this abrogated IFN-γ production. This same effect has been noted in in vitro studies; culture of PBMCs from TB patients with anti-IL-10 alone induced increased IFN-γ, whereas addition of anti-IL-12 abrogated the stimulatory effects of anti-IL-10 (83). Both the experimental and virtual model findings highlight the inherent complexity of efficient immune regulation; depletion of IL-10 before the immune response is initiated may actually facilitate the clearance of bacteria at the cost of tissue damage. Depletion after latency has been achieved pulls the system out of equilibrium into oscillations. Thus, IL-10 is a key regulator of the latent state.

Discussion

In this paper, we have presented a virtual model of the immune response to *M. tuberculosis* that characterizes the cytokine and cellular network that is operational during TB infection. Using this model system, we are able to explore the effects of perturbing different factors in the immune response to TB, including expression of cytokines; activation, deactivation, and recruitment of macrophages; T cell and macrophage effector mechanisms; T cell recruitment and differentiation; as well as bacterial growth. First, the model is able to simulate three disease trajectories: latency; active TB; and reactivation. Using this model we are able to identify which parameters govern the behavior of the system toward the different outcomes; factors affecting macrophage functions (such as activation, infection and bactericidal capabilities) as well as effector T cell functions (cytotoxicity from $CD4^+$ T cells as well as other cells such as $CD8^+$ T cells) must achieve a balance to control infection. However, even if latency is achieved, it may come at the expense of severe tissue damage if the response is not properly controlled. A balance in Th1 and Th2 immune responses governed by IFN-γ, IL-10, and IL-4 facilitate down-regulation of tissue damage. These results are further confirmed through virtual deletion and depletion experiments.

An explanation as to whether or not there is a clear-cut Th1/Th2 switch in TB is complex. Our model indicates that if the immune response is initially and dominantly Th2-type, then the system will proceed to active TB. However, if the system is initially and dominantly Th1-type, the result is not definitive. Suppressing infection is dependent on a number of factors related to the strength of effector cell activity. However, even if latency is achieved, if effector cell function is not tightly regulated, severe tissue damage may occur. Down-regulation is governed by elements of both Th1- and Th2-type responses. If the system achieves latency, does reactivation occur due to a switch in immune control? Our model results show that a weakening in the functional elements of either the Th1- or Th2-type response can lead to reactivation. Thus, a balance in both arms of the helper T cell response are required for successful suppression of infection.

Virtually every study of TB infection ultimately seeks to determine what factors lead to the development of active disease and to understand the immune mechanisms involved in disease resolution. However, very few studies of susceptibility to *M. tuberculosis* infection have considered how subtle variations in the complex interactions between individual components of the human immune response may influence susceptibility to TB. An understanding of these effects is a necessary component in understanding how the complex network of immune cells and cytokine signals governs the clinical outcome in TB infection. Although obvious defects in this network may predispose one to mycobacterial infections, in the majority of cases, subtle defects or variances in the host response play a decisive role in determining which individuals suppress infection with *M. tuberculosis* and which individuals develop active TB.

Recent evidence indicates that other elements of the host-pathogen interaction may be important in the immune response to *M.*

tuberculosis. Data suggest that *CD8*$^+$ T cells are an important source of IFN-γ and may also be significant in killing bacteria, via cytotoxic mechanisms (18, 32, 84, 85). For purposes of the present model, we have elected to include CD8$^+$ T cells indirectly in two ways: by incorporating an exogenous source of IFN-γ; and by accounting for enhanced CTL activity. Also the cytokine TNF-α clearly plays an important but potentially complex role in the host response to *M. tuberculosis* (86), not only by synergizing with IFN-γ in activating macrophages (37, 66) but also by playing a role in the modulation of macrophage apoptosis (20) and granuloma formation (87). Subsequent models by our group directly incorporate both TNF-α and CD8$^+$ T cell effector mechanisms.

As with any experimental system, our conclusions are limited by the assumptions we make. However, a clear strength of the modeling process lies in the ability to quickly and easily compare the effects of including alternate assumptions into the model. With respect to the model system under evaluation, we have considered alternate equation forms at each step of model development, validation, and prediction. We outline below several assumptions that may impact predictions generated by our model.

First, a number of murine studies indicate that the cytokine response to *M. tuberculosis* may tend to be either predominantly Th1 or Th2 at the site of infection in the lung (27). If this is the case, cells that simultaneously secrete both IFN-γ and IL-4 (Th0 cells) may not be seen outside of the lymph node priming site. However, a number of studies in humans provide strong evidence to the contrary (71, 73). Both of these scenarios have been considered in our model development. Additionally, we have modeled the effects of Ag presentation, which typically occurs in the lymph nodes, as occurring at the site of infection. Future studies will specifically investigate the role of this spatial component, and a two-compartment model (lymph node and lung) including the role of dendritic cells and Th0 cells in the lymph node is anticipated. Compartmental models of the lymph system and blood have contributed to a greater understanding of AIDS progression in pediatric patients (88) as well as progression of HIV in adults (89).

Another limitation is reflective of the field of human immunology in general; although one study reports that BAL is reflective of cell populations and cytokine quantities in tissue granulomas (35), to our knowledge, no other studies have specifically addressed the validity of BAL as a quantitative predictor of lung tissue cytokine and cell concentrations. Thus, the possibility exists that immune response in the airspace may differ from that in the interstitium. However, model parameter estimation must be based on experimental results, which are currently limited primarily to BAL measurements in humans. Additionally, a number of studies cite the validity of BAL measurements as a qualitative predictor of lung status and function (33–35, 90–92). However, a strength of the model is that parameter values can easily be updated as new data become available.

Elucidating the immunological mechanisms responsible for the different courses of disease (i.e., latency, fast progression, and reactivation) not only aids in the design of treatment strategies based on traditional chemotherapy but also facilitates the development of new approaches based on immunotherapy. These immunological alternatives may also be used therapeutically, because augmenting present therapy is becoming increasingly important in the face of multidrug-resistant TB. Thus, the model can now be used to explore treatment in both chemo- and immunotherapeutic settings.

Models of the cellular immune response regarding Th1/Th2-type immunity have been published in recent years (e.g., Refs. 93–96). Most are attempts to begin unraveling the complex cytokine and cellular networks in the absence of a specific pathogen invasion. Each argue that models of this type will be necessary in the face of complexity of the networks involved. Models of the host-pathogen interaction with bacteria are even more scarce (97–99). Pilyugin and Antia (96) have explored general mycoparasite-immune dynamic models; however, this paper is the first to explore a detailed immune response to a specific bacterial pathogen. We argue that these reconstructionist (100) models provide an essential complement for approaches used in immunological investigations of TB and other diseases. The synthesis of elements that comprise the complex cytokine and cellular network is necessary to understand how this dynamic system operates as more than the sum of its parts.

Appendix

Parameter estimation

Values for most rate parameters were estimated from published experimental data, with weight given to results obtained from humans or human cells and *M. tuberculosis*-specific data over results based on BCG or other mycobacterial species. We outline below how we incorporate these data into the model. Estimates obtained from multiple studies are presented as a range of values. On those parameters for which we have a range, or those for which no experimental data are available, we performed sensitivity analyses to obtain order of magnitude estimates. Recall from above that our units are cells per milliliter of BAL, and picograms per ml of BAL for cytokines.

Growth and decay rates (α_{19}, α_{20}, μ_{14}, μ_{I12}, μ_{I10}, μ_g). The decay rates of cytokines can be estimated from half-life given by the standard formula

$$r = \frac{\ln 2}{\text{Half-life}}.$$

These values are obtained from experimental results and are summarized in Table III. As an illustration, we derive μ_{I10}, the decay rate of IL-10. When IL-10 was administered i.v. to human volunteers, one study estimated its half-life to be 2.3–3.7 (101). A similar study estimated this quantity to be 2.7–4.5 h (102). Therefore, we estimate a range for $t_{1/2}$ as 2.3–4.5 h, and thus the decay rate of IL-10 lies in the range $3.69/\text{day} \leq \mu_{10} \leq 7.23/\text{day}$. Estimation of μ_{I12}, the decay rate for IL-12 is complicated by the fact that IL-12 is heterodimeric. The half-life for the IL-12 p_{70} heterodimer was estimated to be 14 h in rhesus monkeys (103); we use this as a baseline estimate and explore ranges around the associated decay rate of $\mu_{12} = 1.188/\text{day}$.

Estimates of growth rates for *M. tuberculosis* can be obtained similarly, with bacterial doubling time used in place of cytokine half-life. The doubling time for *M. tuberculosis* may differ depending on the strain used, location of the bacteria (intracellular or extracellular), tissue type, culture conditions, and experimental procedure used to measure growth (104–106). For the *M. tuberculosis* laboratory strain H37Rv, estimates of growth within macrophages vary: 28.6 h (106); 28 h (107); 80–96 h (108) and 36.2 h (104). When measured in tissue (mouse lung), H37Rv was estimated to have a doubling time of 64.2 h (109). Therefore, we estimate the growth rates of intracellular and extracellular *M. tuberculosis* to be $0.17/\text{day} \leq \alpha_{19} \leq 0.594/\text{day}$ and $0.0/\text{day} < \alpha_{20} \leq 0.2591/\text{day}$, respectively.

Baseline cytokine production parameters (α_5, α_{11}, α_{12}, α_8, α_{22}, α_{16}, α_{17}). Ranges for cytokine production levels by various cell lines may be obtained from ELISA either of in vitro cytokine production (57, 58, 60, 110), pleural or BAL fluid from TB patients (50, 111). Results vary due to differences in experimental method, including ELISA used, purity and type of cell line used, estimates of cell concentration in fluid, and stimuli with specific or nonspecific Ag. In addition, cytokine production by T cell lines should be corrected to account for the frequency of Ag-specific cells present. As an illustration, we derive α_5, the rate of production of IFN-γ by Th1 cells. In one study (51), 2.5×10^5/ml human CD4$^+$ T cells were stimulated with live H37Ra *M. tuberculosis* and autologous monocytes. IFN-γ production was measured after 48 h by ELISA and was determined to be 2458 pg/ml $\pm$ 213 pg/ml. An enzyme-linked immunospot assay was used to measure the frequency of IFN-γ-producing cells, determined to be 81/1000. From these measurements, we calculate

$$\alpha_5 = \frac{2458 \text{ pg/ml} \pm 213 \text{ pg/ml}}{2.5 \times 10^5 \text{ cells pg/ml} \times 0.081 \times 2 \text{ days}}$$

or equivalently, that α_5 falls in the range (0.055 pg/cell day, 0.066 pg/cell day). Other experimental results produce similar estimates, giving a final range (0.02 pg/cell day, 0.066 pg/cell day) (50, 56).

Cytokine interaction parameters. In the highly complex cytokine feedback system, some cytokines oppose each other; where one has an up-regulatory effect, the other has a down-regulatory effect. Terms describing these competitive effects between two cytokines on a particular rate are described by cytokine interaction terms (see equations in the next section). Three general types of parameters are estimated for each: a maximum rate; a half-saturation constant; and a relative effect parameter. Their values are summarized in Table IV and outlined below.

Maximal rates (k_6, k_7, k_3, $w\alpha_{10}$ . . .) describe the limiting rate of a process when given maximal stimulation. They are equivalent to the standard V_{max} from Michaelis-Menten kinetics. These values may be obtained from dose-response curves generated from in vitro cytokine assays using cells stimulated by *M. tuberculosis* and varying levels of stimulatory and inhibitory cytokines. Half-saturation constants (s_1–s_6) are equivalent to the standard k_m in Michaelis-Menten kinetics. These values are equal to the concentration of the stimulatory cytokine where the associated rate is half-maximal and can be estimated from these same dose-response curves.

Most cytokines have different concentrations at which their effects are optimal (in picograms per milliliter). For example, IL-12 is typically present in concentrations of 100–200 pg/ml (57, 73, 111), whereas IFN-γ is present in larger amounts, usually around 300 to >1000 pg/ml (50, 72, 73). Relative effect parameters (f_1–f_6) adjust for these difference in values, and we scale for the inhibitory cytokine in each case. These ratios are estimated from cytokine assays of pleural or BAL fluid (50, 72, 73, 111).

Additionally, when one cytokine opposes the effect of another, maximal inhibition may be <100%. Thus, percent inhibition terms (p_i for $i = 1, \cdots 6$) represent the amount of inhibition of the maximal response that occurs when an average level of inhibitory cytokine is present. Values for the p_i are obtained from assays measuring cytokine expression in the presence and absence of the inhibitory cytokine and should be between 0.0 and 1.0. These effects are incorporated into the estimates for the relative effect parameters (f_1, f_2, $\cdots f_6$) and thus are not explicitly written in the modeling terms. As an example, we derive the three parameters associated with the term that governs IL-12 production by macrophages, namely,

$$\alpha_{10}\left(\frac{I_\gamma}{I_\gamma + f_5 I_{10} + s_5}\right).$$

The form of this term follows Michaelis-Menten except for the addition of the $f_5 I_{10}$ in the denominator; this is the inhibition term. One study (56) measured maximal rates of IL-12 (IL-12 p70) production by human macrophages in response to live H37Ra *M. tuberculosis* and IFN-γ by preincubating 2×10^6/ml human macrophages with an excess of IFN-γ and 10 *M. tuberculosis* bacteria per macrophage. IL-12 p70 protein in 24-h supernatants was measured by ELISA to be 55 pg/ml. Dividing by the number of macrophages, we estimate that $\alpha_{10} = 2.75 \times 10^{-5}$ pg/cell day. In contrast, early treatment with an excess of IL-10 correlated with a mean decrease of 57% in IL-12 p70 protein (56). Thus, we would expect that $p_5 > 0.57$. Another study (60) examining the effects of varying doses of IFN-γ on IL-12 production by mouse macrophages reports a dose-response curve yielding an estimate for s_5 in the range $100 < s_5 < 500$. Furthermore, results from pleural fluid ELISA suggest a reasonable effector concentration ratio of IFN-γ to IL-10 to be ~10 (50, 73, 111). From this, we estimate the relative effect parameter $f_5 = 4.8$. Incorporation of results from several other similar studies (58, 59, 111, 112) extend this estimate of f_5 to the range (4.8, 65).

Other saturation parameters. Other saturation parameters occur in terms of Michaelis-Menten form (see equations in the next section), and are presented in Table V. Reasonable ranges for c_{10}, the effect of *M. tuberculosis* inducing IFN-γ production from sources other than $CD4^+$ T cells (such as $CD8^+$ T cells and NK cells) may be inferred from studies measuring this effect in human PBMCs (58). Cell line-specific experimental data are not presently available; however, estimates obtained using PBMCs may be used to determine parameter ranges to explore in further analyses. From a dose-response curve measuring IFN-γ induction vs bacteria/ml, we find that the effect of induction saturates when cells are stimulated with 10^5 bacteria/ml, whereas IFN-γ production was nearly nonexistent in the absence of Ag stimulation. Therefore, we estimate c_{10} lies in the range of 1×10^3–5×10^4 bacteria/ml. Table V summarizes these values.

IL-10 effects on macrophage deactivation may be inferred from the inhibitory effect of IL-10 on IFN-γ production (which is dependent on Ag presentation from activated macrophages). This value can be estimated from dose-response curves yielding s_8 in the range (200 pg/ml, 500 pg/ml). As estimates for IL_{10} at the site of infection tend to be somewhat lower than this estimate (50, 72, 73), we explore the range (100 pg/ml, 500 pg/ml). In the absence of specific experimental data, other IL-10-related terms may be expected to fall into ranges that physiologically relate to the concentration of IL-10. Table IV summarizes these values.

Cell recruitment and death term parameters. Life spans for various cell types can be obtained from literature (113–115). From these values, estimates of cell death rates are derived as 1/life span. Values obtained for these parameters are presented in Table VI.

Estimates for cell recruitment parameters may be obtained from chemotaxis assays (69, 116) and experimental measurements of the number and types of cells to be found in normal and *M. tuberculosis*-infected lung tissue (67–70). Given T cell life spans, we may derive a reasonable estimate for the rate of flow of T lymphocytes from the infection site. Using this value and estimates for T cell counts at the site of infection, it is possible to estimate reasonable ranges for rates of recruitment of cell populations. The rate of recruitment of resting macrophages ($M\Phi$) in the absence of infection (s_M) can be calculated from the uninfected control average of 3–4 $\times$ 10^5 cells/ml (67–69, 117). Assuming that resting macrophages die at rate $\mu_R = 0.011$, to maintain a steady state population, s_M must lie in the interval

$$\frac{330\ M\Phi}{\text{ml day}} \leq s_M \leq \frac{440\ M\Phi}{\text{ml day}}.$$

Growth rates for activated T cells are based on the observation that they divide several times per day (42); we therefore estimate that the doubling time for a $CD4^+$ T cell is in the range 6–12 h, yielding α_2 in the range of (1.4/day, 2.8/day).

Parameters relevant to macrophage activation and deactivation may be derived using data from assays measuring various aspects of activation including up-regulation of MHC II receptors, increases in IFN-γ production (47–49), and increases in rates of mycobacterial killing (36, 118). For instance, expression of MHC II on human *M. tuberculosis*-infected macrophages was measured by flow cytometry after 24 h in the absence and presence of 10 ng/ml of IL-10 (20). The mean fluorescence index in the absence of IL-10 was 730 ± 175; in the presence of IL-10, the mean fluorescence index was 467 ± 175. Because concentrations of cytokine used were well above those found in normal lung tissue, we assume that these values provide a reasonable estimate of maximal rates of macrophage deactivation: $k_4 \approx (467/730) \approx 0.36$.

Approximate rates of Th1/Th2 differentiation and the relative effects of the cytokines IL-12, IFN-γ, and IL-4 can be estimated from intracellular staining followed by flow cytometry (7, 8). Rates of Th0 to Th2 differentiation were measured by stimulating Th0 cells with Ag via APC and 200 U/ml of IL-4 (7). After 7 days, 85% of cells costained for IL-4 and IFN-γ, whereas 14% stained for only IL-4. From these data, we estimate k_7 in the range (0.02/day, 0.7/day).

Effector mechanisms (k_{14}, k_{15}, k_{17}, k_{18}, p, N, c_4). Rates of T cell-mediated cytotoxic activity against infected macrophages may be obtained from cytotoxicity assays (13, 16, 20, 105, 119–122). Cytotoxicity is measured by the formula

Table III. *Cytokine decay rates and* M. tuberculosis *growth rates*

Name	Range	Reference	Definition	Units
μ_{I4}	2.77	103	IL-4 decay rate	1/day
μ_{I12}	1.188	103	IL-12 decay rate	1/day
μ_{I10}	(3.6968, 7.23)	101, 102	IL-10 decay rate	1/day
μ_g	(2.16, 33.27)	127	IFN-γ decay rate	1/day
α_{19}	(0.17, 0.594)	104, 105, 107, 108, 128	Growth rate, intracellular bacteria	1/day
α_{20}	(0.0, 0.2591)	104, 105, 109	Growth rate, extracellular bacteria	1/day

Table IV. *Cytokine production and interaction parameters*

Name	Range	Reference	Definition	Units
α_5	(0.02, 0.066)	50, 51, 56	IFN-γ by T_1	pg/T_1 day
α_7	(0.02, 0.066)	50, 51, 56	IFN-γ by T_0	pg/T_0 day
α_8	8.0×10^{-5}	60, 79, 111	IL-12 by M_A	pg/M_A day
α_{22}	8.0×10^{-5}	60, 79, 111	IL-12 by M_I	pg/M_I day
α_{11}	(2.8×10^{-3}, 9.12×10^{-3})	16	IL-4 by T_0	pg/T_0 day
α_{12}	(2.18×10^{-2}, 9.12×10^{-2})	16	IL-4 by T_2	pg/T_2 day
α_{16}	(2.0×10^{-4}, 1.0×10^{-3})	53, 55	IL-10 by T_1	pg/T_1 day
α_{17}	(2.0×10^{-4}, 6.0×10^{-3})	53, 55	IL-10 by T_2	pg/T_2 day
α_{10}	(2.75×10^{-5}, 2.75×10^{-4})	56, 56, 60, 111	Max[a] IL-12 from M_R	pg/M_R day
α_{18}	(2.0×10^{-3}, 6×10^{-3})	53, 55	Max IL-10 by T_0	pg/T_0 day
α_{13}	(1.1×10^{-3}, 1.25×10^{-3})	51, 56, 59	Max IL-10 from M_R	pg/M_R day
α_{14}	(1.1×10^{-3}, 1.25×10^{-3})	51, 56, 59	Max IL-10 from M_A	pg/M_A day
s_g	(360, 730)	16, 51, 129	Max IFN_γ from $CD8^+$ and NK	pg/ml day
s_1	(50, 110)	Estimated	Half-sat, IFN-γ on T_0 to T_1	pg/ml
s_2	(1, 2)	Estimated	Half-sat, IL-4 on T_0 to T_2	pg/ml
s_3	(50, 110)	Estimated	Half-sat, IFN-γ on MΦ activation	pg/ml
s_4	(50, 100)	64, 112	Half-sat, IL-12 on IFN-γ	pg/ml
s_5	(100, 500)	60	Half-sat, IFN-γ on IL-12	pg/ml
s_6	(51, 58)	130, estimated	Half-sat, IL-10, IFN-γ on IL-10	pg/ml
s_7	(5, 100)	64	Half-sat, IL-12 on NK, $CD8^+$ IFN-γ	pg/ml
s_8	(100, 500)	20	Half-sat, IL-10 on M_A deactivation	pg/ml
s_9	100	53, 54	Half-sat, IL-12 on IL-10	pg/ml
f_1	(2.9, 410)	79	Adjustment, IL-4/IFN-γ on T_0 to T_1	Scalar
f_2	(0.0012, 0.16)	79	Adjustment, IFN-γ/IL-4 on T_0 to T_2	Scalar
f_4	(0.76, 3.2)	52, 79	Adjustment, IL-10/IL-12 on IFN-γ	Scalar
f_5	(4.8, 65)	59, 60, 79, 112	Adjustment, IL-10/IFN-γ on IL-12	Scalar
f_6	(0.025, 0.053)	59, 79, 130	Adjustment, IFN-γ, IL-10 on IL-10	Scalar

[a] Max, Maximal; Half-sat, half-saturated; MΦ, macrophage.

$$k_{14} = \frac{\text{Experimental release } {}^{51}\text{Cr} - \text{spontaneous release } {}^{51}\text{Cr}}{\text{Maximal release } {}^{51}\text{Cr} - \text{spontaneous release } {}^{51}\text{Cr}}$$

Using this assay, reported rates for *CD4*$^+$ T cell-mediated lysis of macrophages range from 0.5 (119), 0.6 (15), and 0.4 (16). This estimate represents killing by $CD4^+$ T cells. Similar estimates were obtained for $CD8^+$ T cells, ranging from 1.0 (17), to 0.3 (15, 123). Because $CD8^+$ T cells are not directly included in the model, we sum the values for $CD8^+$ T cell cytotoxicity with the $CD4^+$ estimates to include their effects indirectly.

Estimating the rate-activated macrophages kill *M. tuberculosis* (k_{15}) is complicated by several considerations including: type of model system (murine vs human), type of bacteria used (*Mycobacterium avium-cellulase*, BCG, H37Ra, H37Rv), and the fact that bactericidal effects of activated macrophages have been shown to be dependent on the presence of lymphocytes as well as IFN-γ, making it difficult to distinguish whether killing is due solely to activated macrophages. Therefore, we have derived estimates from available data (6, 37, 124) and used these estimates as a basis for parameter exploration over a range. Depending on the value for k_{14} (the maximal rate of cytotoxicity of T cells on infected macrophages) the value of $k_{15} > 4.5 \times 10^{-7}$ ml/cell/day, leads to latency (see Table I).

To estimate N (the maximum MOI of chronically infected macrophages), values of per-macrophage bacterial counts were obtained (108, 125). We take the upper limit of observed counts in the range of 50 to 100 bacteria/cell to be the maximal carrying capacity of infected macrophages (N).

Evidence suggests that TB inhibits apoptosis of its host cell primarily via induction of IL-10 (19, 20, 121, 126). Therefore, TUNEL assay for apoptosis in the presence of varying doses of IL-10, and in the absence of IL-10 (by using anti-IL-10) is a reasonable method for quantifying p, the TB-mediated inhibition of macrophage apoptosis. Using this method, ~15% of cells registered as TUNEL positive in the presence of 20 ng/ml, whereas in the absence of IL-10 nearly 50% were TUNEL positive. Therefore, $(1 - p) = (15/50) = 0.3$, implying $p = 0.7$. Table VII summarizes these parameter estimates.

Model equations

We model human TB infection at the site of infection in the lung by tracking the interactions between two bacterial populations, six cell populations, and four cytokines using nonlinear, ordinary differential equations to describe rates of change. These 12 populations are placed into 4 groups: 1) macrophages; 2) $CD4^+$ T lymphocytes; 3) cytokines; and 4) bacteria. Note that $T_T(t) = T_0(t) + T_1(t) + T_2(t)$ represents the total activated $CD4^+$ T cell population, and $B_T(t) = B_E(t) + w \cdot B_I(t)$, where $0 \leq w \leq 1$. This accounts for the possibility that intracellular bacteria make a diminished contribution to overall Ag stimulation because they are within chronically infected macrophages. Unless experimental data or mechanistic considerations indicate otherwise, all effects mediated by bacterial Ag are assumed to be a function

Table V. *Other bacterial and macrophage-related saturation parameters*

Name	Range	Reference	Definition	Units
c_8	(5×10^4, 5×10^5)	37	Half-sat,[a] bacteria on M_R activation	B_T/ml
c_9	(1×10^6, 1×10^7)	Estimated	Half-sat, bacteria on chronic infection	B_E/ml
c_{10}	(1×10^3, 5×10^4)	58	Half-sat, bacteria on IFN-γ by $CD8^+$	B_T/ml
c_{12}	(1×10^3, 5×10^5)	Estimated	Half-sat, total bacteria IL-10 by M_R	B_T/ml
c_{14}	(1×10^4, 1×10^5)	Estimated	Half-sat M_A on IFN-γ by $CD4^+$	M_A/ml
c_{15}	(1×10^4, 1×10^5)	Estimated	Half-sat M_A on T_0 proliferation	M_A/ml
c_{18}	(5×10^4, 5×10^5)	56, 58	Half-sat, bacteria on IL-12 by M_R	B_T/ml
c_{28}	(1.5×10^5, 1.5×10^6)	131	Half-sat, bacteria on M_R recruitment by M_R	B_T/ml

[a] Half-sat, Half-saturated.

Table VI. *Cell recruitment death and differentiation term parameters*

Name	Range	Reference	Definition	Units
α_1	0.05	116, estimated	Max[a] T_0 cell recruitment	T_0 /MΦ day
α_2	(1.4, 2.8)	42	Max growth rate for T_0	1/day
α_3	0.0528	116, estimated	Max T_1/T_2 recruitment	T/MΦ day
α_4	(0.03, 0.05)	Estimated	M_R recruitment by M_A, M_I	1/day
α_{21}	(0.01, 0.07)	131, estimated	Max M_R recruitment by M_R	1/day
s_M	(330, 430)	67–70, 117	M_R source	MΦ/ml day
μ_a	0.011	132	Death rate, M_A	1/day
μ_r	0.011	132	Death rate, M_R	1/day
μ_I	0.011	132	Death rate, M_I	1/day
μ_{da}	(0.3, 2.0)	Estimated	Deactivation rate, M_A	1/day
μ_{T_0}	0.3333	114	Death rate, T_0	1/day
μ_{T_1}	0.3333	114	Death rate, T_1	1/day
μ_{T_2}	0.3333	114	Death rate, T_2	1/day
k_6	$(2.9 \times 10^{-4}, 1.0 \times 10^{-3})$	8, 62	Max T_0 to T_1 rate	ml/pg day
k_7	(0.02, 0.7)	8, 62	Max T_0 to T_2 rate	1/day
k_2	(0.2, 0.4)	Estimated	Chronic infection rate	1/day
k_3	(0.2, 0.4)	Estimated	M_R activation rate	1/day
k_4	(0.36, 0.4)	20	M_A deactivation by IL-10	1/day

[a] Max, Maximal.

of $B_T(t)$. Although quantities are time dependent, t notation has been suppressed for ease of presentation and that within equations, the appearance of the parameter ϵ represents a small positive constant to keep the denominator bounded away from zero. Each population in the model is time dependent, but we suppress the '(t)' notation for ease of readability.

Macrophage dynamics. Equations describing macrophage dynamics during *M. tuberculosis* infection are given by

$$\frac{dM_R}{dt} = s_M + \alpha_4(M_A + wM_I) + \alpha_{21}M_R\left(\frac{B_T}{B_T + c_{28}}\right) + k_4M_A\left(\frac{I_{10}}{I_{10} + s_8}\right) - k_2M_R\left(\frac{B_E}{B_E + c_9}\right) - k_3M_R\left(\frac{I_\gamma}{I_\gamma + s_3}\right)\left(\frac{B_T}{B_T + c_8}\right) + \mu_{da}M_A\left(\frac{s_3}{I_\gamma + s_3}\right)\left(\frac{c_8}{B_T + c_8}\right) - \mu_rM_R \quad (1)$$

$$\frac{dM_A}{dt} = k_3M_R\left(\frac{I_\gamma}{I_\gamma + s_3}\right)\left(\frac{B_T}{B_T + c_8}\right) - k_4M_A\left(\frac{I_{10}}{I_{10} + s_8}\right) - \mu_{da}M_A\left(\frac{s_3}{I_\gamma + s_3}\right)\left(\frac{c_8}{B_T + c_8}\right) - \mu_aM_A \quad (2)$$

$$\frac{dM_I}{dt} = k_2M_R\left(\frac{B_E}{B_E + c_9}\right) - k_{17}M_I\left(\frac{B_I^m}{B_I^m + (N\,M_I)^m + \epsilon}\right) - k_{14}M_I\left(\frac{T_T/M_I}{(T_T/M_I) + c_4}\right)\left(1 - p\,\frac{B_I}{B_I + N\,M_I + \epsilon}\right) - \mu_IM_I \quad (3)$$

For the resting macrophage population, there is both a source of new cells coming into the site (s_M) and death of cells that stay the remainder of their life span ($-\mu_rM_R$). With no infection, the macrophage population should remain at the equilibrium value $\bar{M}_R = s_M/\mu_r$. This is reasonable, in that macrophages die and are replaced by new macrophages from the blood even in the absence of infection. When bacteria are present, additional resting macrophages are recruited to the site of infection in the lung in response to chemokines released by activated and infected macrophages at rates α_4 and $w\alpha_4$ (where $0 < w < 1$), respectively, and by resting macrophages when exposed to Ag, at maximal rate α_{21}.

On reaching the site of infection, resting macrophages may become activated in response to IFN-γ (I_γ) and exposure to Ag, at a maximum rate of k_3, giving a loss term for Equation 1 and a gain term for Equation 2. Unless they are given further stimulation by IFN-γ and Ag, activated macrophages revert to the resting state, at rate μ_{da}. Activated macrophages may also be deactivated by IL-10, at a maximal rate k_4, and undergo natural death, at rate μ_a.

Resting macrophages that are unable to clear their bacterial load may become chronically infected, at maximal rate k_2. Chronic infection of a macrophage may result in death of the cell; the rate of this process is determined by the number of bacteria living within chronically infected macrophages ($B_I(t)$) relative to the number of chronically infected host cells ($M_I(t)$). Assuming that the average maximal per macrophage carrying capacity (MOI) is N, then the carrying capacity for the entire population of chronically infected macrophages is given by $N\,M_I(t)$. When the number of intracellular bacteria ($B_I(t)$) is near $N\,M_I(t)$, we assume that approximately one-half of the chronically infected macrophages will contain bacterial numbers exceeding their maximal carrying capacity of N. Thus, the rate of death due to infection itself will be one-half of the maximum rate k_{17} (the mathematical form of this term is discussed in more detail below for Equations 11 and 12). Chronically infected macrophages may be eliminated via apoptosis by $CD4^+$ T cells, at a maximal rate of k_{14}. Both $CD8^+$ T cells (indirectly) and $CD4^+$ T cells (directly) account for the cytotoxic effects. The actual rate of this effect will depend on the E:T ratio, $T_T(t)$:$M_I(t)$, and is half-maximal when this ratio is equal to c_4. Finally, we assume the intracellular TB population ($B_I(t)$) is capable of opposing the death of its host cell; this effect is represented by

Table VII. *Parameters involved in T cell effector mechanisms*

Name	Range	Reference	Definition	Units
c_4	(5, 20)	13, 16, 105	Half-sat,[a] T_T to M_I ratio for M_I lysis	T_T/M_I
k_{14}	(0.7, 1.6)	14–16, 105	Max T cell lysis of M_I	1/day
k_{17}	(0.05, 0.5)	120	Max M_I death due to bacteria	1/day
k_{15}	1.25×10^{-7}	37	Max killing of bacteria by M_A	ml/M_A day
k_{18}	$(1.25 \times 10^{-9}, 1.25 \times 10^{-8})$	37	Max killing of bacteria by M_R	ml/M_R day
p	0.7	126	Max % inhibition of apoptosis	
N	(50, 100)	106, 108, 125	Max MOI of M_I	B_I/M_I

[a] Half-sat, Half-saturated; Max, maximal.

$$1 - p\left(\frac{B_I}{B_I + N\,M_I + \epsilon}\right)$$

where p denotes the maximal percent effect of $B_I(t)$ on this process.

Cytokine dynamics. Equations describing the rate changes of the four cytokines in the model are given are as follows. Each equation is comprised of terms accounting for cytokine production from different cell lines as well as cytokine half-life.

$$\frac{dI_\gamma}{dt} = s_g\left(\frac{B_T}{B_T + c_{10}}\right)\left(\frac{I_{12}}{I_{12} + s_7}\right) + \alpha_5 T_1\left(\frac{M_A}{M_A + c_{14}}\right) + \alpha_7\left(\frac{I_{12}}{I_{12} + f_4 I_{10} + s_4}\right)\left(\frac{M_A}{M_A + c_{14}}\right)T_0 - \mu_g I_\gamma \tag{4}$$

$$\frac{dI_{12}}{dt} = \alpha_8 M_A + \alpha_{22} M_I + \alpha_{10}\left(\frac{I_\gamma}{I_\gamma + f_5 I_{10} + s_5}\right)\left(\frac{B_T}{B_T + c_{18}}\right)M_R - \mu_{I12} I_{12} \tag{5}$$

$$\frac{dI_{10}}{dt} = \left(\alpha_{13} M_R\left(\frac{B_T}{B_T + c_{12}}\right) + \alpha_{14} M_A\right)\left(\frac{s_6}{I_{10} + f_6 I_\gamma + s_6}\right) + \alpha_{16} T_1 + \alpha_{17} T_2 + \alpha_{18} T_0\left(\frac{I_{12}}{I_{12} + s_9}\right) - \mu_{I10} I_{10} \tag{6}$$

$$\frac{dI_4}{dt} = \alpha_{11} T_0 + \alpha_{12} T_2 - \mu_{I4} I_4 \tag{7}$$

IFN-γ is produced by Th1 cells at rate α_5, and by Th0 cells at maximal rate α_7 in response to Ag presentation by activated macrophages. Production of IFN-γ by Th0 cells is enhanced by IL-12 with saturable kinetics and is opposed by IL-10. Actual levels of production are dependent on the relative levels of IL-12 and IL-10. Finally, IFN-γ decays at rate μ_g. Other sources of IFN-γ, including NK cells and $CD8^+$ T cells, are also believed to play a role in TB infection. Because these cells are not accounted for in the model directly at present, we include the source term, s_g, to account for this extra production. This source is a function of the bacterial concentration and IL-12, implying that the degree of infection and IL-12 stimulation governs this extra source (26, 75).

IL-12 is produced by activated macrophages at rate α_8, by infected macrophages at rate α_{22}, and by resting macrophages up to maximal rate α_{10} in response to *M. tuberculosis*. This production is enhanced by IFN-γ and is opposed by IL-10.

IL-10 is produced primarily by resting and activated macrophages. Resting macrophages produce IL-10 at maximal rate α_{13} after phagocytosing (or other interactions with) *M. tuberculosis*. This production is opposed by both IFN-γ and IL-10 itself. To capture this effect, we denote baseline production of IL-10 by infected macrophages as $\alpha_{13} M_R(t)$. Since IL-10 or IFN-γ inhibit this production (either individually or jointly), this inhibition is represented by

$$-\alpha_{13}\frac{I_{10} + f_6 I_\gamma}{I_{10} + f_6 I_\gamma + s_6},$$

where s_6 represents the Michaelis-Menten half-saturation constant for IL-10 and IFN-γ inhibition of IL-10 production. Together this process is then written as

$$\alpha_{13} M_R - \alpha_{13}\left(\frac{I_{10} + f_6 I_\gamma}{I_{10} + f_6 I_\gamma + s_6}\right)M_R = \alpha_{13}\left(\frac{s_6}{I_{10} + f_6 I_\gamma + s_6}\right)M_R.$$

To account for Ag exposure inducing IL-10 production by resting macrophages, we append the entire term by

$$\left(\frac{B_T}{B_T + c_{12}}\right).$$

Although macrophages are a primary source of IL-10, it is also produced by all three subsets of $CD4^+$ T lymphocytes, at rate α_{16} by Th1 cells and α_{17} for Th2 cells. Production of IL-10 from Th0 cells is dependent on IL-12 up to a maximal rate α_{18}.

Finally, IL-4 is produced by Th0 cells at rate α_{11} and by Th2 cells at rate α_{12}. IL-4 has a known half-life, decaying at rate μ_4.

$CD4^+$ T lymphocyte dynamics.

$$\frac{dT_0}{dt} = \alpha_1(M_A + wM_I) + \alpha_2 T_0\left(\frac{M_A}{M_A + c_{15}}\right) - \mu_{T0} T_0 - k_6\left(\frac{I_\gamma}{I_\gamma + f_1 I_4 + s_1}\right)I_{12} T_0 - k_7\left(\frac{I_4}{I_4 + f_2 I_\gamma + s_2}\right)T_0 \tag{8}$$

$$\frac{dT_1}{dt} = \alpha_3(M_A + wM_I) + k_6\left(\frac{I_\gamma}{I_\gamma + f_1 I_4 + s_1}\right)I_{12} T_0 - \mu_{T1} T_1 \tag{9}$$

$$\frac{dT_2}{dt} = \alpha_3(M_A + wM_I) + k_7\left(\frac{I_4}{I_4 + f_2 I_\gamma + s_2}\right)T_0 - \mu_{T2} T_2 \tag{10}$$

T cells arrive at the site of infection either as fully differentiated Th1 or Th2 cells or as Th0 cells. Their recruitment is induced in response to signals released by infected and activated macrophages. The net rate of Th0 cell migration per signaling macrophage is α_1, whereas the corresponding rate for fully differentiated Th1 and Th2 cells is α_3.

On arrival to the site of infection, Th0 cells may undergo further rounds of proliferation in response to stimulation by activated macrophages, up to maximal rate α_2. Th0 cells differentiate into either Th1 or Th2 cells, where Th1 differentiation is enhanced by IFN-γ and IL-12, up to maximal rate k_6, and is opposed by IL-4. The rate of Th1 differentiation is half-maximal when the concentration of IFN-γ is s_1. Conversely, if Th0 cells are stimulated by IL-4, they are induced to differentiate to Th2 cells, at maximal rate k_7. This rate is half-maximal when the concentration of IL-4 reaches s_2. Th2 differentiation is opposed by IFN-γ. Finally, all three classes of T cells have a finite lifetime and die at rates μ_{T0}, μ_{T1}, μ_{T2}, respectively.

Bacterial dynamics. Equations describing the interactions and growth of *M. tuberculosis* are given by

$$\frac{dB_E}{dt} = \alpha_{20} B_E - k_{15} M_A B_E - k_{18} M_R B_E + \mu_I B_I + k_{17} N\,M_I\left(\frac{B_I^m}{B_I^m + (N\,M_I)^m + \epsilon}\right) - k_2\left(\frac{N}{2}\right)M_R\left(\frac{B_E}{B_E + c_9}\right) \tag{11}$$

$$\frac{dB_I}{dt} = \alpha_{19} B_I\left(1 - \frac{B_I^m}{B_I^m + (N\,M_I)^m + \epsilon}\right) - k_{17} N\,M_I\left(\frac{B_I^m}{B_I^m + (N\,M_I)^m + \epsilon}\right) + k_2\left(\frac{N}{2}\right)M_R\left(\frac{B_E}{B_E + c_9}\right) - k_{14} N\,M_I\left(\frac{T_T/M_I}{(T_T/M_I) + c_4}\right)\left(1 - p\,\frac{B_I}{B_I + N\,M_I + \epsilon}\right) - \mu_I B_I \tag{12}$$

Extracellular bacteria (B_E) grow at maximal rate α_{20}. They are killed by either activated or resting macrophages at rates k_{15} and k_{18}, respectively. Exchange terms between the intracellular and extracellular compartments closely parallel terms describing the dynamics of the infected macrophage population (see Equation 2). Intracellular bacteria (B_I) become extracellular when their host macrophage is killed via the infection and not via the CTL response. Assuming each infected macrophage carries up to N bacteria, the term describing this effect is the same as the corresponding macrophage term except that the maximal rate for the bacteria is N times the maximal rate for the host population (or $k_{17}N$). Extracellular bacteria become intracellular when their host macrophage becomes chronically infected. We assume that such a macrophage carries approximately one-half of its carrying capacity, or $N/2$ bacteria, and therefore the maximal rate for the bacterial dynamic is given by $k_2\,N/2$. Natural life spans of chronically infected macrophages are modeled separately from cytotoxic terms, and exchange of bacteria between extracellular and intracellular compartments due to this dynamic is modeled via the term $\mu_I B_I$.

Dynamics of bacteria existing within the intracellular environment of a chronically infected macrophage are described by the second equation. Intracellular bacteria may continue to grow in an unregulated manner, eventually causing the death of their host macrophage. Alternatively, it has been suggested that bacterial growth may be limited in some manner (44), presumably as numbers within an individual cell approach the maximal carrying capacity. We incorporate and test the latter assumption into the term describing intracellular bacterial growth,

$$\alpha_{19} B_I\left(1 - \frac{B_I^m}{B_I^m + (N\,M_I)^m + \epsilon}\right).$$

We estimate the value of the exponent $m = 2$. Growth occurs at or near the maximal rate of α_{19} until the intracellular bacterial population size reaches

the carrying capacity (given by $N M_I$) of the chronically infected macrophage population. When this capacity is reached, bacterial growth is sharply reduced. The mathematical form of this term describes a sigmoidal curve, based on the form of a Hill equation:

$$\frac{B_I^m}{B_I^m + (N M_I)^m + \epsilon}.$$

Finally, intracellular bacteria are assumed to be killed when their host macrophage is lysed via a T cell-mediated defense mechanism; we assume that N intracellular bacteria are killed for each macrophage that is eliminated, giving a loss term with maximal rate $k_{14}N$.

Acknowledgments

We thank Dr. JoAnne Flynn for helpful discussions, Drs. Vic DiRita and Gary Huffnagle for critical readings of the manuscript, and Eliza Peterson for technical assistance.

References

1. Comstock, G. W. 1982. Epidemiology of tuberculosis. *Am. Rev. Respir. Dis. 125:8.*
2. Canetti, G. *The Tubercle Bacillus in the Pulmonary Lesion in Man.* Springer Publishing Co., New York, 1955.
3. Myrvik, Q. N., E. S. Leake, and M. J. Wright. 1984. Disruption of phagosomal membranes of normal alveolar macrophages by the H37Rv strain of *Mycobacterium tuberculosis. Am. Rev. Respir. Dis. 129:322.*
4. McDonough, K., Y. Kress, and B. R. Bloom. 1993. Pathogenesis of tuberculosis: interaction of *Mycobacterium tuberculosis* with macrophages. *Infect. Immun. 61:2763.*
5. Armstrong, J. A., and P. D. Hart. 1971. Response of cultured macrophages to *Mycobacterium tuberculosis*, with observations on fusion of lysosomes and phagosomes. *J. Exp. Med. 134:713.*
6. Bonecini-Almeida, G. M., S. Chitale, I. Boutsikakis, J. Geng, H. Doo, S. He, and J. L. Ho. 1998. Induction of in vitro human macrophage anti-*M. tuberculosis* activity: requirement for IFN-γ and primed lymphocytes. *J. Immunol. 160:4490.*
7. Openshaw, P., E. E. Murphy, N. A. Hosken, V. Maino, K. Davis, K. Murphy, and A. O'Garra. 1995. Heterogeneity of intracellular cytokine synthesis at the single cell level in polarized T helper 1 and T helper 2 populations. *J. Exp. Med. 182:1357.*
8. Assenmacher, M., M. Lohning, A. Scheffold, S. Richter, J. Miltenyi, J. Schmitz, and A. Radbruch. 1998. Commitment of individual Th1-like lymphocytes to expression of IFN-γ vs IL-4 and IL-10. *J. Immunol. 161:2825.*
9. Palmer, E. M., and G. A. van Seventer. 1997. Human T helper cell differentiation is regulated by the combined action of cytokines and accessory cell-dependent costimulatory signals. *J. Immunol. 15:2654.*
10. Nakamura, T., R. K. Lee, S. Y. Nam, E. R. Podack, K. Bottomly, and R. A. Flavell. 1997. Roles of IL-4 and IFN-γ in stabilizing the T helper cell type 1 and 2 phenotype. *J. Immunol. 158:2648.*
11. Maggi, E., P. Parronchi, R. Manetti, C. Simonelli, M. Piccinni, F. Rugiu, M. De Carli, M. Ricci, and S. Romagnani. 1992. Reciprocal regulatory effects of IFN-γ and IL-4 on the in vitro development of human Th1 and Th2 clones. *J. Immunol. 148:2142.*
12. Vergelli, M., B. Hemmer, P. A. Muraro, L. Tranquill, W. E. Biddison, A. Sarin, H. F. McFarland, and R. Martin. 1997. Human autoreactive CD4$^+$ T cell clones use perforin- or Fas/Fas ligand-mediated pathways for target cell lysis. *J. Immunol. 158:2756.*
13. Oddo, M., T. Renno, A. Attinger, T. Bakker, H. R. MacDonald, and P. R. Meylan. 1998. Fas ligand-induced apoptosis of infected human macrophages reduces the viability of intracellular *Mycobacterium tuberculosis. J. Immunol. 160:5448.*
14. Lewisohn, D. M., T. T. Bement, J. Xu, D. Lynch, K. H. Grabstein, S. G. Reed, and M. R. Alderson. 1998. Human purified protein derivative-specific CD4$^+$ T cells use both CD95-dependent and CD95-independent cytolytic mechanisms. *J. Immunol. 160:2374.*
15. Tan, J. S., D. H. Canaday, W. H. Boom, K. N. Balaji, S. K. Schwander, and E. A. Rich. 1997. Human alveolar T lymphocyte responses to *Mycobacterium tuberculosis* antigens: role for CD4$^+$ and CD8$^+$ cytotoxic T cells, and relative resistance of alveolar macrophages to lysis. *J. Immunol. 159:290.*
16. Tsukaguchi, K., K. N. Balaji, and W. H. Boom. 1995. CD4$^+$ $\alpha\beta$ T cell and $\gamma\delta$ T cell responses to *Mycobacterium tuberculosis. J. Immunol. 154:1786.*
17. Skinner, M. A., S. Yuan, R. Prestidge, D. Chuk, J. D. Watson, and P. L. J. Tan. 1997. Immunization with heat-killed *Mycobacterium vaccae* stimulates CD8$^+$ cytotoxic T cells specific for macrophages infected with *Mycobacterium tuberculosis. Infect. Immun. 65:4525.*
18. Lalvani, R., R. Brookes, R. J. Wilkinson, A. S. Malin, A. A. KPathan, P. Andersen, H. Dockrell, G. Pasvol, and A. V. S. Hill. 1998. Human cytolytic and interferon γ-secreting T lymphocytes specific for *Mycobacterium tuberculosis. Proc. Natl. Acad. Sci. USA 95:270.*
19. Balcewicz-Sablinska, M., J. Keane, H. Kornfeld, and H. G. Remold. 1998. Pathogenic *Mycobacterium tuberculosis* evades apoptosis of host macrophages by release of TNF-R2, resulting in inactivation of TNF-α. *J. Immunol. 161:2636.*
20. Rojas, M., M. Olivier, P. Gros, L. F. Barrera, and L. F. Garcia. 1999. TNF-α and IL-10 modulate the induction of apoptosis by virulent *Mycobacterium tuberculosis* in murine macrophages. *J. Immunol. 162:6122.*
21. Keane, J., H. G. Remold, and H. Kornfeld. 2000. Virulent *Mycobacterium tuberculosis* strains evade apoptosis of infected alveolar macrophages. *J. Immunol. 164:2016.*
22. Altare, F., A. Durandy, D. Lammas, J. Emile, S. Lamhamedi, F. Deist, P. Drysdale, E. Jouanguy, R. Doffinger, F. Bernaudin, et al. 1998. Impairment of mycobacterial immunity in human interleukin-12 receptor deficiency. *Science 80:1432.*
23. North, R. J., R. LaCourse, L. Ryan, and P. Gros. 1999. Consequence of *Nramp1* deletion to *Mycobacterium tuberculosis* infection in mice. *Infect. Immun. 67:5811.*
24. Flynn, J. L., M. M. Goldstein, K. J. Triebold, J. Sypek, S. Wolf, and B. R. Bloom. 1995. IL-12 increases resistance of BALB/c mice to *Mycobacterium tuberculosis* infection. *J. Immunol. 155:2515.*
25. Flynn, J. L., J. Chan, K. J. Triebold, D. K. Dalton, T. A. Stewart, and B. R. Bloom. 1993. An essential role for interferon-γ in resistance to *Mycobacterium tuberculosis* infection. *J. Exp. Med. 178:2249.*
26. Cooper, A., J. Magram, J. Ferrante, and I. Orme. 1997. Interleukin-12 (IL-12) is crucial to the development of protective immunity in mice intravenously infected with *Mycobacterium tuberculosis. J. Exp. Med. 186:39.*
27. Lin, Y., M. Zhang, F. M. Hofman, J. Gong, and P. F. Barnes. 1996. Absence of a prominent Th2 cytokine response in human tuberculosis. *Infect. Immun. 64:1351.*
28. North, R. J. 1998. Mice incapable of making IL-4 and IL-10 display normal resistance in infection with *Mycobacterium tuberculosis. Clin. Exp. Immunol. 113:2827.*
29. Fenhalls, G., A. Wong, J. Bezuidenhout, P. V. Helden, P. Bardin, and P. T. Lukey. 2000. In situ production of γ interferon, interleukin-4, and tumor necrosis factor α mRNA in human lung tuberculous granuloma. *Infect. Immun. 68:2827.*
30. Caruso, A. M., N. Serbina, E. Klein, J. K. Triebold, B. R. Bloom, and J. L. Flynn. 1999. Mice deficient in CD4 T cells have only transiently diminished levels of IFNγ, yet succumb to tuberculosis. *J. Immunol. 162:540.*
31. Scanga, C. A., V. P. Mohan, H. Joseph, K. Yu, J. Chan, and J. L. Flynn. 1999. Reactivation of latent tuberculosis: variations on the Cornell murine model. *Infect. Immun. 67:5431.*
32. Serbina, N. V., and J. L. Flynn. 1999. Early emergence of CD8$^+$ T cells primed for production of type 1 cytokines in the lungs of *Mycobacterium tuberculosis*-infected mice. *Infect. Immun. 67:3980.*
33. Ainslie, G. M., J. A. Solomon, and E. D. Bateman. 1992. Lymphocyte and lymphocyte subset numbers in blood and in bronchoalveolar lavage and pleural fluid in various forms of human pulmonary tuberculosis at presentation and during recovery. *Thorax 47:513.*
34. Moodley, Y. P., T. Dorasamy, S. Venketasamy, V. Naicker, and U. G. Lalloo. 2000. Correlation of CD4:CD8 ratio and tumour necrosis factor TNF-α levels in induced sputum with bronchoalveolar lavage fluid in pulmonary sarcoidosis. *Thorax 55:696.*
35. Law, K. F., J. Jagirdar, M. Weiden, and W. N. Rom. 1996. Tuberculosis in HIV-positive patients: cellular response and immune activation in the lung. *Am. J. Respir. Crit. Care Med. 153:1377.*
36. Nathan, C. F., H. W. Murray, M. E. Wiebe, and B. Y. Rubin. 1983. Identification of interferon-γ as the lymphokine that activates human macrophage oxidative metabolism and antimicrobial activity. *J. Exp. Med. 158:670.*
37. Flesch, I., and S. Kaufmann. 1990. Activation of tuberculostatic macrophage functions by γ interferon, interleukin-4, and tumor necrosis factor. *Infect. Immun. 58:2675.*
38. Stout, R. D., and K. Bottomly. 1989. Antigen-specific activation of effector macrophages by IFN-γ producing Th1 T cell clones. *J. Immunol. 142:760.*
39. Koppelman, B., J. J. Neefjes, J. E. de Vries, and R. de Waal Malefyt. 1997. IL-10 downregulates MHC class II $\alpha\beta$ peptide complexes at the plasma membrane of monocytes by affecting arrival and recycling. *Immunity 7:861.*
40. Gazinelli, R. T., I. P. Oswald, S. L. James, and A. Sher. 1992. IL-10 inhibits parasite killing and nitrogen oxide production by IFNγ-activated macrophages. *J. Immunol. 148:1792.*
41. Murray, P. J., L. Wang, C. Onufryk, R. I. Tepper, and R. A. Young. 1997. T-cell derived IL-10 antagonizes macrophage function in mycobacterial infection. *J. Immunol. 158:315.*
42. Janeway, C. A., and P. Travers. *Immunobiology: The Immune System in Health and Disease.* Current Biology Ltd./Garland Publishing, New York, 1997.
43. Sturgill-Koszycki, S., P. H. Schlesinger, P. Chakraborty, P. L. Haddix, H. L. Collins, A. K. Fok, R. D. Allen, S. L. Gluck, J. Heuser, and D. G. Russell. 1994. Lack of acidification in *Mycobacterium* phagosomes produced by exclusion of the vesicular proton-ATPase. *Science 263:678.*
44. Shankar, S., C. E. Barry, and J. T. Belisle. 2000. Identification and characterization of peptides that modulate the growth of *Mycobacterium tuberculosis*. In *ASM Conference on Tuberculosis: Past, Present, and Future, June 20–24,* New York, (Abstr. 228).
45. de Waal Malefyt, R., J. Haanen, H. Spits, M. Roncarlo, A. teVelde, C. Figdor, K. Johnson, R. Kastelein, H. Yssel, and J. E. deVries. 1991. Interleukin 10 and viral IL-10 strongly reduce antigen-specific human T cell proliferation by diminishing the antigen-presenting capacity of monocytes via downregulation of class II MHC complex expression. *J. Exp. Med. 174:915.*
46. Del Prete, G., M. Almerigogna, and M. Giudizi. 1993. Human IL-10 is produced by both type 1 helper (Th1) and type 2 helper (Th2) T cell clones and inhibits their antigen-specific proliferation and cytokine production. *J. Immunol. 150:353.*

47. Malefyt, R., J. Abrams, B. Bennett, C. G. Figdor, and J. E. de Vries. 1991. Interleukin 10 (IL-10) inhibits cytokine synthesis by human monocytes: an autoregulatory role of IL-10 produced by monocytes. *J. Exp. Med. 174:1209.*
48. Fiorentino, D. F., A. Zlotnik, T. R. Mosmann, M. Howard, and A. O-Garra. 1991. IL-10 inhibits cytokine production by activated macrophages. *J. Immunol. 147:3815.*
49. Fiorentino, D. F., A. Zlotnik, T. R. Mosmann, M. Howard, and A. O-Garra. 1991. IL-10 acts on the antigen-presenting cell to inhibit cytokine production by Th1 cells. *J. Immunol. 146:3444.*
50. Barnes, P. F., S. Lu, J. S. Abrams, E. Wang, M. Yamamura, and R. L. Modlin. 1993. Cytokine production at the site of disease in human tuberculosis. *Infect. Immun. 61:3482.*
51. Tsukaguchi, K., B. de Lange, and W. H. Boom. 1999. Differential regulation of IFN-γ, TNF-α, and IL-10 production by $CD4^+$ $\alpha\beta$ TCR^+ T cells and $V\delta2^+$ T cells in response to monocytes infected with *Mycobacterium tuberculosis*-H37Ra. *Cell. Immunol. 194:12.*
52. Othieno, C., C. S. Hirsch, B. Hamilton, K. Wilkinson, J. J. Ellner, and Z. Toosi. 1999. Interaction of *Mycobacterium tuberculosis*-induced transforming growth factor β1 and interleukin-10. *Infect. Immun. 67:5730.*
53. Meyaard, L., E. Hovenkamp, S. A. Otto, and F. Miedma. 1996. IL-12-induced IL-10 production by human T cells as a negative feedback for IL-12-induced immune responses. *J. Immunol. 156:2776.*
54. Peng, X., A. Kasran, and J. L. Ceuppens. 1997. Interleukin 12 and B7/CD28 interaction synergistically upregulate IL-10 production by human T cells. *Cytokine 9:499.*
55. Yssel, H., R. de Waal Malefyt, M. Roncarolo, J. S. Abrams, R. Lahesmaa, H. Spits, and J. E. de Vries. 1992. IL-10 is produced by subsets of human $CD4^+$ T cell clones and peripheral blood T cells. *J. Immunol. 149:2378.*
56. Fulton, R., J. V. Cross, Z. T. Toosi, and W. H. Boom. 1998. Regulation of interleukin-12 by interleukin-10, transforming growth factor-β, tumor necrosis factor-α, and interferon-γ in human monocytes infected with *Mycobacterium tuberculosis* H37Ra. *J. Infect. Dis. 178:1105.*
57. Ladel, C. H., G. Szalay, D. Riedel, and S. H. E. Kaufmann. 1997. Interleukin-12 secretion by *Mycobacterium tuberculosis*-infected macrophages. *Infect. Immun. 65:1936.*
58. Fulton, S. A., J. M. Johnson, S. F. Wolf, D. S. Sieburth, and W. H. Boom. 1996. Interleukin-12 production by human monocytes infected with *Mycobacterium tuberculosis*: role of phagocytosis. *Infect. Immun. 64:2523.*
59. Isler, P., B. Galve de Rochemonteix, F. Songeon, N. Boehringer, and L. P. Nicod. 1999. Interleukin-12 production by human alveolar macrophages is controlled by the autocrine production of interleukin-10. *Am. J. Respir. Cell Mol. Biol. 20:270.*
60. Chensue, S. W., J. H. Ruth, K. Warmington, P. Lincoln, and S. L. Kunkel. 1995. In vivo regulation of macrophage IL-12 production during type 1 and type 2 cytokine-mediated granuloma formation. *J. Immunol. 155:3546.*
61. Manetti, R., P. Parronchia, M. Giudizi, M. Piccinni, E. Maggi, G. Trinchieri, and S. Romagnani. 1993. Natural killer cell stimulatory factor (interleukin 12 (IL-12)) induces T helper type 1 (Th1)-specific immune responses and inhibits the development of IL-4-producing Th cells. *J. Exp. Med. 177:1199.*
62. Sornasse, T., P. V. Lareas, K. A. Davis, J. E. deVries, and H. Yssel. 1996. Differentiation and stability of T helper 1 and 2 cells derived from naive neonatal $CD4^+$ T cells analyzed at the single cell level. *J. Exp. Med. 184:473.*
63. O'Garra, A. 1998. Cytokines induce the development of functionally heterogeneous T helper cell subsets. *Immunity 8:275.*
64. O'Donnell, M. A., Y. Luo, X. Chen, A. Szilvasi, S. E. Hunter, and S. K. Clinton. 1999. Role of IL-12 in the induction and potentiation of IFNγ in response to bacillus Calmette-Guérin. *J. Immunol. 163:4246.*
65. Szabo, S. J., A. S. Dighe, U. Gubler, and K. M. Murphy. 1997. Regulation of the IL-12R β2 subunit expression in developing Th1 and Th2 cells. *J. Exp. Med. 185:817.*
66. Sato, K., T. Akaki, and H. Tomika. 1998. Differential potentiation of antimycobacterial activity and reactive nitrogen intermediate-producing ability of murine peritoneal macrophages activated by interferon-γ and tumor necrosis factor α. *Clin. Exp. Immunol. 112:63.*
67. Law, K., M. Weiden, T. Harkin, K. Tchou-Wong, C. Chi, and W. L. Rom. 1996. Increased release of interleukin-1β, interleukin-6, and tumor necrosis factor-α by bronchoalveolar cells lavaged from involved sites in pulmonary tuberculosis. *Am. J. Respir. Crit. Care Med. 153:799.*
68. Condos, R., W. N. Rom, Y. M. Liu, and N. W. Schluger. 1998. Local immune responses correlate with presentation and outcome in tuberculosis. *Am. J. Respir. Crit. Care Med. 157:729.*
69. Antony, V. B., S. W. Godbey, S. L. Kunkel, J. W. Hott, D. L. Hartman, M. D. Burdick, and R. M. Strieter. 1993. Recruitment of inflammatory cells to the pleural space. *J. Immunol. 151:7216.*
70. Schwander, S. K., M. Torres, E. Sada, C. Carranza, E. Ramos, M. Tary-Lehmann, R. S. Wallis, J. Sierra, and E. A. Rich. 1998. Enhanced responses to *Mycobacterium tuberculosis* antigens by human alveolar lymphocytes during active pulmonary tuberculosis. *J. Infect. Dis. 178:1434.*
71. Gerosa, F., C. Nisii, S. Righetti, R. Micciolo, M. Marchesini, A. Cazzadori, and G. Trinchieri. 1999. $CD4^+$ T cell clones producing both interferon-γ and interleukin-10 predominate in bronchoalveolar lavages of active pulmonary tuberculosis patients. *Clin. Immunol. 92:224.*
72. Giosue, S., M. Casarini, L. Alemanno, G. Galluccio, P. Mattia, G. Pedicelli, L. Rebek, A. Bisetti, and F. Ameglio. 1998. Effects of aerosolized interferon-α in patients with pulmonary tuberculosis. *Am. J. Respir. Crit. Care Med. 158:1156.*
73. Casarini, M., F. Ameglio, L. Alemanno, P. Zangrilli, P. Mattia, G. Paone, A. Bisetti, and S. Giosue. 1999. Cytokine levels correlate with a radiologic score in active pulmonary tuberculosis. *Am. J. Respir. Crit. Care Med. 159:143.*
74. Cooper, A., D. K. Dalton, T. A. Stewart, J. P. Griffin, D. G. Russell, and I. A. Orme. 1993. Disseminated tuberculosis in IFN-γ gene disrupted mice. *J. Exp. Med. 178:2243.*
75. Wakeham, J., J. Wang, J. Magram, K. Croitoru, R. Harkness, P. Dunn, A. Zganiacz, and Z. Xing. 1998. Lack of both types 1 and 2 cytokines, tissue inflammatory responses, and immune protection during pulmonary infection by *Mycobacterium bovis* bacille Calmette-Guérin in IL-12 deficient mice. *J. Immunol. 160:6101.*
76. Seah, G. T., G. M. Scott, and G. A. W. Rook. 2000. Type 2 cytokine gene activation and its relationship to extent of disease in patients with tuberculosis. *J. Infect. Dis. 181:385.*
77. van Crevel, R., E. Karyadi, F. Preyers, M. Leenders, B. Kullberg, R. Nelwan, and J. van der Meer. 2000. Increased production of interleukin 4 by $CD4^+$ and $CD8^+$ T cells from patients with tuberculosis is related to the presence of pulmonary cavities. *J. Infect. Dis. 181:1194.*
78. Taha, R. A., T. C. Kotsimbos, Y. L. Song, D. Menzies, and D. Hamid. 1997. IFN-γ and IL-12 are increased in active compared to inactive tuberculosis. *Am. J. Respir. Crit. Care Med. 155:1135.*
79. Zhang, M., Y. Lin, D. Iyer, J. Gong, J. S. Abrams, and P. F. Barnes. 1995. T-cell cytokine responses in human infection with *Mycobacterium tuberculosis. Infect. Immun. 63:3231.*
80. Newport, M. J., C. M. Huxley, S. Huston, C. M. Hawrylowicz, B. A. Oostra, R. Williamson, and M. Levin. 1996. A mutation in the interferon-γ-receptor gene and susceptibility to mycobacterial infection. *N. Engl. J. Med. 335:1941.*
81. Jouanguy, E., F. Altare, S. Lamhamedi, P. Revy, J. F. Emile, M. Newport, M. Leven, S. Blanche, J. L. Gaillard, and J. L. Casanova. 1996. Interferon γ receptor deficiency in an infant with fatal Bacille Calmette Guérin infection. *N. Engl. J. Med. 335:1956.*
82. Murray, P. J., and R. A. Young. 1999. Increased antimycobacterial immunity in interleukin-10 deficient mice. *Infect. Immun. 67:3087.*
83. Gong, J. H., M. Zhang, R. L. Modlin, P. S. Linsley, D. Iyer, Y. Lin, and P. F. Barnes. 1996. Interleukin-10 downregulates *Mycobacterium tuberculosis*-induced Th1 responses and CTLA-4 expression. *Infect. Immun. 64:913.*
84. Xing, Z., J. Wang, K. Croitoru, and J. Wakeham. 1998. Protection by CD4 or CD8 T cells against pulmonary *Mycobacterium bovis* bacillus Calmette-Guérin infection. *Infect. Immun. 66:5537.*
85. Smith, S. M., A. S. Malin, T. Pauline, P. T. Lukey, S. E. Atkinson, J. Content, K. Huygen, and H. M. Dockrel. 1999. Characterization of human *Mycobacterium bovis* bacille Calmette-Guérin-reactive $CD8^+$ T cells. *Infect. Immun. 67:5223.*
86. Flynn, J. L., M. M. Goldstein, J. Chan, K. J. Triebold, K. Pfeffer, C. J. Lowenstein, R. Screiber, T. W. Mak, and B. R. Bloom. 1995. Tumor necrosis factor-α is required in the protective immune response to *Mycobacterium tuberculosis* in mice. *Immunity 2:561.*
87. Bean, A. G., D. R. Roach, H. Briscoe, M. P. France, H. Korner, J. D. Sedgwick, and W. J. Britton. 1999. Structural deficiencies in granuloma formation in TNF gene-targeted mice underlie the heightened susceptibility to aerosol *Mycobacterium tuberculosis* infection which is not compensated for by lymphotoxin. *J. Immunol. 162:3504.*
88. Kirschner, D., R. Mehr, and A. Perelson. 1998. The role of the thymus in pediatric HIV-1 infection. *J. Acquired Immune Defic. Syndr. Hum. Retrovirol. 18:95.*
89. Kirschner, D., G. F. Webb, and M. Cloyd. 2000. A model of HIV-1 disease progression based on virus-induced homing and homing-induced apoptosis of $CD4^+$ lymphocytes. *J. Acquired Immune Defic. Syndr. Hum. Retrovirol. 24: 352.*
90. Suzuki, K., N. Tamura, A. Iwase, T. Dambara, and S. Kira. 1996. Prognostic value of Ia^+ T lymphocytes in bronchoalveolar lavage fluid in pulmonary sarcoidosis. *Am. J. Respir. Crit. Care Med. 154:707.*
91. Goldstein, R. A., P. K. Rohatgi, E. H. Bergofsky, E. R. Block, R. P. Daniele, D. R. Dantzker, G. S. Davis, G. W. Hunninghake, T. E. King, Jr., W. J. Metzger, et al. 1990. Clinical role of bronchoalveolar lavage in adults with pulmonary disease. *Am. Rev. Respir. Dis. 142:481.*
92. Rizvi, N., N. A. Rao, and M. Hussain. 2000. Yield of gastric lavage and bronchial wash in pulmonary tuberculosis. *Int. J. Tuberc. Lung Dis. 4:147.*
93. Burke, M. A., B. F. Morel, T. B. Oriss, J. Bray, S. A. McCarthy, and P. A. Morel. 1997. Modeling the proliferative response of T cells to IL-2 and IL-4. *Cell. Immunol. 178:42.*
94. Fishman, M. A., and A. S. Perelson. 1994. Th1/Th2 cross regulation. *J. Theor. Biol. 170:25.*
95. Segel, L. A., and R. L. Bar-Or. 1999. On the role of feedback in promoting conflicting goals of the adaptive immune system. *J. Immunol. 163:1342.*
96. Pilyugin, S., and R. Antia. 2000. Modeling immune responses with handling time. *Bull. Math. Biol. 62:869.*
97. Kirschner, D. 1999. Dynamics of coinfection with *M. tuberculosis* and HIV-1. *Theor. Popul. Biol. 55:94.*
98. Kirschner, D., and R. Freter. 2000. Mathematical models of colonization and persistence in bacterial infections. *Persistent Bacterial Infections*. ASM Press, Washington, DC, pp. 79–99.
99. Falk, P., A. Syder, J. L. Guruge, D. Kirschner, M. J. Blaser, and J. I. Gordon. 2000. Theoretical and experimental approaches for studying factors defining the *Helicobacter pylori*-host relationship. *Trends Microbiol. 8:321.*
100. Savageau, M. 1991. Reconstructionist molecular biology. *New Biol. 3:190.*

101. Huhn, R. D., E. Radwanski, S. M. O'Connell, M. G. Sturgill, L. Clarke, R. P. Cody, M. B. Affrime, and D. L. Cutler. 1996. Pharmacokinetics and immunomodulatory properties of intravenously administered recombinant human interleukin-10 in healthy volunteers. *Blood 87:699.*
102. Huhn, R. D., E. Radwanski, J. Gallo, M. B. Affrime, R. Sabo, G. Gonyo, A. Monge, and D. L. Cutler. 1997. Pharmacodynamics of subcutaneous recombinant human interleukin-10 in healthy volunteers. *Clin. Pharmacol. Ther. 62:171.*
103. Remick, D., and J. S. Freidland. *Cytokines in Health and Disease.* 2nd Ed. Marcel Dekker, New York, 1997.
104. Silver, R. F., Q. Li, and J. J. Ellner. 1998. Expression of virulence of *Mycobacterium tuberculosis* within human monocytes: virulence correlates with intracellular growth and induction of tumor necrosis factor-α but not with evasion of lymphocyte-dependent monocyte effector functions. *Infect. Immun. 66:1190.*
105. Silver, R. F., A. Li, W. H. Boom, and J. J. Ellner. 1998. Lymphocyte-dependent inhibition of growth of virulent *Mycobacterium tuberculosis* H37Rv within human monocytes: requirement for $CD4^+$ T cells in purified protein-positive, but not in purified protein derivative-negative subjects. *J. Immunol. 160:2408.*
106. Zhang, M., J. Gong, Y. Lin, and P. Barnes. 1998. Growth of virulent and avirulent *Mycobacterium tuberculosis* strains in human macrophages. *Infect. Immun. 66:794.*
107. Manca, M., L. Tsenova, C. E. Barry, A. Bergtold, S. Freeman, P. A. J. Haslett, J. M. Musser, V. H. Freedman, and G. Kaplan. 1999. *Mycobacterium tuberculosis* CDC1551 induces a more vigorous host response in vivo and in vitro, but is not more virulent than other clinical isolates. *J. Immunol. 162:6740.*
108. Paul, S., P. Laochumroonvoranpong, and G. Kaplan. 1996. Comparable growth of virulent and avirulent *Mycobacterium tuberculosis* in human macrophages in vitro. *J. Infect. Dis. 174:105.*
109. North, R. J., and A. A. Izzo. 1993. Mycobacterial virulence: virulent strains of *Mycobacterium tuberculosis* have faster in vivo doubling times and are better equipped to resist growth-inhibiting functions of macrophages in the presence and absence of specific immunity. *J. Exp. Med. 177:1723.*
110. Orme, I. M., A. D. Roberts, J. P. Griffin, and J. S. Abrams. 1993. Cytokine secretion by CD4 T lymphocytes acquired in response to *Mycobacterium tuberculosis* infection. *J. Immunol. 151:518.*
111. Zhang, M., M. K. Gately, E. Wang, J. Gong, S. F. Wolf, S. Lu, R. Modlin, and P. F. Barnes. 1994. Interleukin 12 at the site of disease in human tuberculosis. *J. Clin. Invest. 93:1733.*
112. D'Andrea, A., M. Aste-Amezaga, N. M. Valiante, X. Ma, M. Kubin, and G. Trinchieri. 1993. Interleukin 10 inhibits human lymphocyte IFN-γ production by suppressing natural killer cell stimulatory factor/IL-12 release. *J. Exp. Med. 178:1041.*
113. Tough, D. F., and J. Sprent. 1995. Lifespan of lymphocytes. *Immunology 14:1.*
114. Sprent, J., and A. Basten. 1973. Circulating T and B lymphocytes of the mouse: lifespans. *Cell. Immunol. 7:40.*
115. Sprent, J. 1993. Lifespans of naive, memory and effector lymphocytes. *Curr. Opin. Immunol. 5:433.*
116. Pace, E., M. Gjomarkaj, M. Melis, M. Profita, M. Spatafora, A. M. Vignola, G. Bonsignore, and C. H. Mody. 1999. Interleukin-8 induces lymphocyte chemotaxis into the pleural space. *Am. J. Respir. Crit. Care Med. 159:1592.*
117. Meddows-Taylor, S., D. J. Martin, and C. T. Tiemessen. 1999. Dysregulated production of interleukin 8 in individuals infected with human immunodeficiency virus type 1 and *Mycobacterium tuberculosis. Infect. Immun. 67:1251.*
118. Chan, J., Y. Xing, R. S. Magliozzo, and B. R. Bloom. 1992. Killing of virulent *Mycobacterium tuberculosis* by reactive nitrogen intermediates produced by activated murine macrophages. *J. Exp. Med. 175:1111.*
119. Placido, R., G. Mancino, A. Amendola, F. Mariani, S. Veddetti, M. Piacentini, A. Sanduzzi, M. L. Bocchino, M. Zembala, and V. Colizza. 1997. Apoptosis of human monocytes in *Mycobacterium tuberculosis* infection. *J. Pathol. 181:31.*
120. Rojas, M., L. F. Barrera, G. Puzo, and L. F. Garcia. 1997. Differential induction of apoptosis by virulent *Mycobacterium tuberculosis* in resistant and susceptible murine macrophages. *J. Immunol. 159:1352.*
121. Keane, J., M. Balcewicz-Sablinska, H. G. Remold, G. L. Chupp, B. B. Meek, M. J. Fenton, and H. Kornfeld. 1997. Infection by *Mycobacterium tuberculosis* promotes human alveolar macrophage apoptosis. *Infect. Immun. 65:298.*
122. Kumararatne, D. S., A. S. Pithie, P. Drysdale, J. S. H. Gaston, R. Kiessling, P. B. Iles, C. J. Ellis, J. Innes, and R. Wise. 1990. Specific lysis of mycobacterial antigen-bearing macrophages by class II MHC-restricted polyclonal T cell lines in healthy donors or patients with tuberculosis. *Clin. Exp. Immunol. 80:314.*
123. Serbina, N., C. C. Liu, C. A. Scanga, and J. L. Flynn. 2000. $CD8^+$ CTL from lungs of *Mycobacterium tuberculosis*-infected mice express perforin in vivo and lyse infected macrophages. *J. Immunol. 165:353.*
124. Schaible, U. E., S. Sturgill-Koszycki, P. H. Schlesinger, and D. G. Russell. 1998. Cytokine activation leads to acidification and increases in maturation of *Mycobacterium avium* complex containing phagosomes in murine macrophages. *J. Immunol. 160:1290.*
125. Hirsch, C. S., J. J. Ellner, D. G. Russell, and E. A. Rich. 1994. Complement receptor-mediated uptake and tumor necrosis factor-α-mediated growth inhibition of *Mycobacterium tuberculosis* by human alveolar macrophages. *J. Immunol. 152:743.*
126. Balcewicz-Sablinska, M., H. Gan, and H. G. Remold. 1999. Interleukin 10 produced by macrophages inoculated with *Mycobacterium avium* attenuates mycobacteria-induced apoptosis by reduction of TNF-α activity. *J. Infect. Dis. 180:1230.*
127. Kurzrock, R., M. G. Rosenblum, S. A. Sherwin, A. Rios, M. Talpaz, J. R. Quesada, and J. U. Gutterman. 1985. Pharmacokinetics, single-dose tolerance, and biological activity of recombinant γ-interferon in cancer patients. *Cancer Res. 45:2866.*
128. Zhang, M., J. Gong, Z. Yang, B. Samten, D. Cave, and P. F. Barnes. 1999. Enhanced capacity of a wide spread strain of *Mycobacterium tuberculosis* to grow in human macrophages. *J. Infect. Dis. 179:1213.*
129. Westermann, J., and R. Pabst. 1992. Distribution of lymphocyte subsets and natural killer cells in the human body. *J. Clin. Invest. 70:539.*
130. Chomarat, P., M. Rissoan, J. Banchereau, and P. Miossec. 1993. Interferon-γ inhibits interleukin 10 production by monocytes. *J. Exp. Med. 177:523.*
131. Sadek, M. I., E. Sada, Z. Toosi, S. K. Schwander, and E. A. Rich. 1998. Chemokines induced by infection of mononuclear phagocytes with mycobacteria and present in lung alveoli during active pulmonary tuberculosis. *Am. J. Respir. Cell Mol. Biol. 19:513.*
132. Van Furth, R., M. Diesselhoff-Den Dulk, and H. Mattie. 1973. Quantitative study on the production and kinetics of mononuclear phagocytes during an acute inflammatory reaction. *J. Exp. Med. 138:1315.*